Contents lists available at ScienceDirect

Deep-Sea Research Part I

Nutrient fluxes, oxygen consumption and fatty acid composition from deep-water demo- and hexactinellid sponges from New Zealand

Tanja Stratmann [a,b,c,*], Kathrin Busch [d], Anna de Kluijver [c], Michelle Kelly [e], Sadie Mills [f], Sven Rossel [g], Peter J. Schupp [h,i]

[a] Department of Ocean Systems, NIOZ – Royal Netherlands Institute for Sea Research, Landsdiep 4, 1797 SZ, 't Horntje, (Texel), the Netherlands
[b] Department of Estuarine & Delta Systems, NIOZ – Royal Netherlands Institute for Sea Research, Korringaweg 7, 4401 NT, Yerseke, the Netherlands
[c] Department of Earth Sciences, Faculty of Geosciences, Utrecht University, Vening Meineszgebouw A, Princetonlaan 8a, 3584 CB, Utrecht, the Netherlands
[d] Division of Marine Ecology, Marine Symbioses, GEOMAR Helmholtz-Centre for Ocean Research, Düsternbrooker Weg 20, 24105, Kiel, Germany
[e] National Centre for Coasts and Oceans, National Institute of Water and Atmospheric Research, 41 Market Place Viaduct Harbour, 1010, Auckland, New Zealand
[f] NIWA Invertebrate Collection, National Institute of Water and Atmospheric Research, 301 Evans Bay Parade Hataitai, 6021, Wellington, New Zealand
[g] Senckenberg am Meer, German Centre for Marine Biodiversity Research (DZMB), Südstrand 44, 26382, Wilhelmshaven, Germany
[h] Institute for Chemistry and Biology of the Marine Environment, Carl von Ossietzky University of Oldenburg, Schleusenstraße 1, 26382, Wilhelmshaven, Germany
[i] Helmholtz Institute for Functional Marine Biodiversity at the University of Oldenburg (HIFMB), Ammerländer Heerstrasse 231, D-26129, Oldenburg, Germany

ARTICLE INFO

ABSTRACT

Sponges are an important component of deep-water ecosystems enhancing eukaryotic biodiversity by hosting diverse endo- and epibiota and providing three dimensional habitats for benthic invertebrates and fishes. As holobionts they are important hosts of microorganisms which are involved in carbon and nitrogen cycling. While increasing exploration of deep-water habitats results in new sponge species being discovered, little is known about their physiology and role in nutrient fluxes. Around New Zealand (Southwest Pacific), the sponge biodiversity is particularly high, and we selected six deep-sea sponge genera (*Saccocalyx*, *Suberites*, *Tedania*, *Halichondria/Dendoricella*, *Lissodendoryx*) and a member of the Sceptrulophora order for *in-situ* and *ex-situ* experiments.

We investigated the biochemical composition of the sponges, measured oxygen consumption and inorganic nutrient fluxes, as well as bacterial and phospholipid-derived fatty acid (PLFA) compositions. Our aim was to assess differences in fluxes and fatty acid composition among sponges and linking their bacterial communities to nitrogen cycling processes.

All sponges excreted nitrite and ammonia. Nitrate and phosphate excretion were independent of phylum affiliation (Demospongiae, Hexactinellida). Nitrate was excreted by *Halichondria/Dendoricella* and *Lissodendoryx*, whereas *Suberites*, *Tedania*, and Sceptrulophora consumed it. Phosphate was excreted by Sceptrulophora and *Halichondria/Dendoricella* and consumed by all other sponges. Oxygen consumption rates ranged from 0.17 to 3.56 ± 0.60 mmol O_2 g C^{-1} d^{-1}.

The PLFA composition was very sponge-genera dependent and consisted mostly of long-chain fatty acids. Most PLFAs were sponge-specific, followed by bacteria-specific PLFAs, and others.

All sponges, except for *Suberites*, were low-microbial abundance (LMA) sponges whose bacterial community composition was dominated by Proteobacteria, Bacteroidota, Planctomycetota, and Nitrospinota. *Suberites* consisted of high-microbial abundance (HMA) sponges with Proteobacteria, Chloroflexota, Acidobacteriota, and Actinobacteriota as dominant bacteria.

Based on the inorganic nitrogen flux measurements, we identified three types of nitrogen cycling in the sponges: In type 1, sponges (*Dendoricella* spp. indet., *Lissodendoryx*) respired aerobically and ammonified organic matter (OM) to ammonium, fixed N_2 to ammonium, and nitrified aerobically heterotrophically produced ammonium to nitrate and nitrite. In type 2, sponges (*Halichondria* sp., Sceptrulophora, *Suberites*, *Tedania*) respired OM aerobically and ammonified it to ammonium. They also reduced nitrate anaerobically to

* Corresponding author. Department of Estuarine & Delta Systems, NIOZ – Royal Netherlands Institute for Sea Research, Korringaweg 7, 4401 NT, Yerseke, the Netherlands.

E-mail address: tanja.stratmann@nioz.nl (T. Stratmann).

ammonium via dissimilatory nitrate reduction to ammonium. In type 3, ammonium was microbially nitrified to nitrite and afterwards to nitrate presumably by ammonium-oxidizing Bacteria and/or Archaea.

1. Introduction

Sponges (phylum Porifera) are the evolutionary oldest metazoans on our planet (Feuda et al., 2017; Müller et al., 2007; Simion et al., 2017) and important members of benthic ecosystems (Bell, 2008). In the Queen Charlotte Basin at the western continental shelf of Canada (NE Pacific), for instance, glass sponges (class Hexactinellida) form sponge reef complexes with a total area of 182 km^2 and a maximum reef height of 21 m (Conway et al., 2005). Radiocarbon dating of mollusk shells indicated that these reef complexes are between 1430 ± 50 and 5700 ± 60 years old (Conway et al., 1991). They host a diverse megafauna, including crustaceans, such as crabs, shrimps, prawns, and euphausiids, and rockfish (Conway et al., 2001). In soft-sediment abyssal plains, glass sponge stalks can be considered "habitat islands" that provide hard substrate for other deep-sea epifauna (Beaulieu, 2001). The analysis of 2418 sponge stalks in photographs taken at Station M (NE Pacific) revealed that all epifauna were facultative suspension feeders that belonged mostly to zoanthids, tunicates, ophiuroids, and actinarians (Beaulieu, 2001). In tropical coral reefs, sponges are often the most diverse benthic phylum and in Caribbean coral reefs, they belong to the four organism groups with the largest areal coverage besides algae, scleractinian corals, and octocorals (Diaz and Rützler, 2001). In open reef habitats that are exposed to light, sponges cover up to 24% of the hard substrate (Zea, 1993), whereas in cryptic sub-rubble habitats that receive less light, they cover up to 54% of the area (Meesters et al., 1991).

Depending on their biomass, sponges contribute significantly to benthic respiration. It was estimated that the deep-sea sponge *Geodia barretti* Bowerbank, 1858 population in the 300 km^2 large Træna Marine Protected Area (Norwegian continental shelf) respires 60 t carbon (C) d^{-1} (Kutti et al., 2013). In fact, the entire sponge ecosystem at the Norwegian continental shelf is estimated to respire 306,000 tC yr^{-1} (Cathalot et al., 2015). Furthermore, in oligotrophic areas, sponges can also be important sources of nitrogen (N) (Bell, 2008). Sponges in Mediterranean sublittoral rocky bottom habitats were estimated to release 2.5–7.9 mmol N m^{-1} d^{-1} (Jiménez and Ribes, 2007), whereas at Marion Lagoon (Western Australia), Keesing et al. (2013) calculated a N release by sponges of 0.35–0.63 mmol N m^{-1} d^{-1}. This corresponds to 10–18% of the recycled N in the oligotrophic west Australian continental shelf (Keesing et al., 2013).

Sponges are holobionts (Webster and Taylor, 2012) consisting of the sponge itself and a microbial community that can contribute up to 38% to the overall sponge holobiont volume (Vacelet, 1975). Based on the density of microorganisms present in the sponge holobiont, they are classified as either high-microbial-abundance (HMA) sponges or low microbial abundance (LMA) sponges (Hentschel et al., 2003). In shallow waters, LMA sponges contain typically around 10^5 to 10^6 bacteria g^{-1} sponge tissue which is comparable to the density of microorganisms in seawater, whereas HMA sponges typically host around 10^8 to 10^{10} microorganisms g^{-1} sponge tissue (Hentschel et al., 2006). The microbiome of shallow-water LMA sponges is often dominated by one Bacteria phylum (Giles et al., 2013), whereas the microbiome of shallow-water HMA sponges consists of a more diverse bacterial community (Erwin et al., 2015; Moitinho-Silva et al., 2017). Among others, they are Chloroflexota hotspots (Bayer et al., 2018). In the deep sea, LMA glass sponges (Hexactinellida) host a microbiome with a different taxonomic composition compared to the microbiome of LMA demosponges, HMA sponges or the microbial community in reference water samples (Busch et al., 2022; Steinert et al., 2020).

Fatty acids are components of lipids and serve as source of energy (Lindsay, 1975) and building blocks of membranes (Spector and Yorek,

1985; van Deenen, 1966). Furthermore, they are important for transducing signals in cells (Faergeman and Knudsen, 1997; Graber et al., 1994) and for the regulation of gene expression (Sampath and Ntambi, 2004). As several fatty acids can only be synthesized by specific taxa, these may be used as dietary tracers and provide information about diet preferences and food origin (Kelly and Scheibling, 2012). Bacteria, for instance, produce fatty acids with iso (*i*) and ante-iso (*ai*)-branched carbon (C) chains, such as *i*-C15:0, *ai*-C15:0, *i*-C17:0, and *ai*-C17:0 (Kaneda, 1991). Sponges, in comparison, produce long chain fatty acids ($\geq$C24) via elongation of shorter chain fatty acids they take up as part of their diet (Carballeira et al., 1986; de Kluijver et al., 2021). These fatty acids are known as "demospongic acids" because they were first discovered in demosponges (Litchfield et al., 1976), though they are also present in glass sponges, but not in calcareous sponges (Lawson et al., 1984; Schreiber et al., 2006). As sponge holobionts consist of both, sponge cells and microorganisms, the fatty acid composition of sponges usually includes bacteria- and sponge-specific fatty acids (e.g., Bart et al., 2020; de Kluijver et al., 2021; Morganti et al., 2022; Rix et al., 2016; van Duyl et al., 2020).

In this study, we measured *in-situ* and *ex-situ* oxygen and inorganic nutrient fluxes in deep-sea sponges (595–4161 m water depth) around New Zealand in the Southeast Pacific. New Zealand belongs to the "temperate Australasia" biogeographic realm (Spalding et al., 2007) which has one of the highest sponge biodiversities (1361 sponge species (Kelly and Sim-Smith, 2023; Spalding et al., 2007; Van Soest et al., 2012). In fact, habitat suitability modeling predicts that demosponges and hexactinellid sponges may occur mostly along the continental margin of New Zealand, whereupon hexactinellid sponges may also find favorable habitats on the Chatham Rise (Georgian et al., 2019). These areas are part of the exclusive economic zone of New Zealand, which is about 21 times larger than the terrestrial part of the country (Macdiarmid et al., 2013). It provides different regulatory, provisioning, and non-consumptive ecosystem services (Macdiarmid et al., 2013) and sponges could be an undervalued contributor to these ecosystem services, particularly to regulating (i.e., nutrient regeneration, biological habitat formation) and supporting ecosystem services (i.e., nutrient cycling, secondary production, biodiversity) (Thurber et al., 2014).

We investigated whether oxygen and nutrient fluxes differed between sponge clusters (i.e., sponges for which a species level distinction was not possible based on DNA barcoding and MALDI-TOF MS), and we tried to link bacterial communities in sponges with inorganic nutrient fluxes to decipher dominant nitrogen cycling processes inside the sponges. Furthermore, we assessed differences in the fatty acid composition among the various sponge clusters. All these data will help to better understand the ecosystem services which sponges provide around New Zealand and to support conservation efforts protecting the sponges.

2. Materials and methods

2.1. In-situ incubation experiment

During R/V *Sonne* cruise SO254 around New Zealand (Fig. 1) in January and February 2017, a sponge ($n = 1$: TS001, Fig. 2, Table 1, Fig. S1) was incubated *in-situ* at 4161 m in a 50 $\times$ 50$\times$ 50 cm large benthic incubation chamber (the so-called "CUBE" (Stratmann et al., 2018)) for 5 h. For this purpose, the CUBE was placed over the sponge by the remotely operated vehicle ROV Kiel 6000 (GEOMAR, Kiel, Germany) and water samples (~35 ml) were taken automatically every hour for the measurement of inorganic nutrient concentrations (nitrate, nitrite, ammonium, phosphate). Oxygen concentration (μmol O$_2$ kg^{-1} seawater) was recorded continuously every 10 s by an oxygen optode (Contros
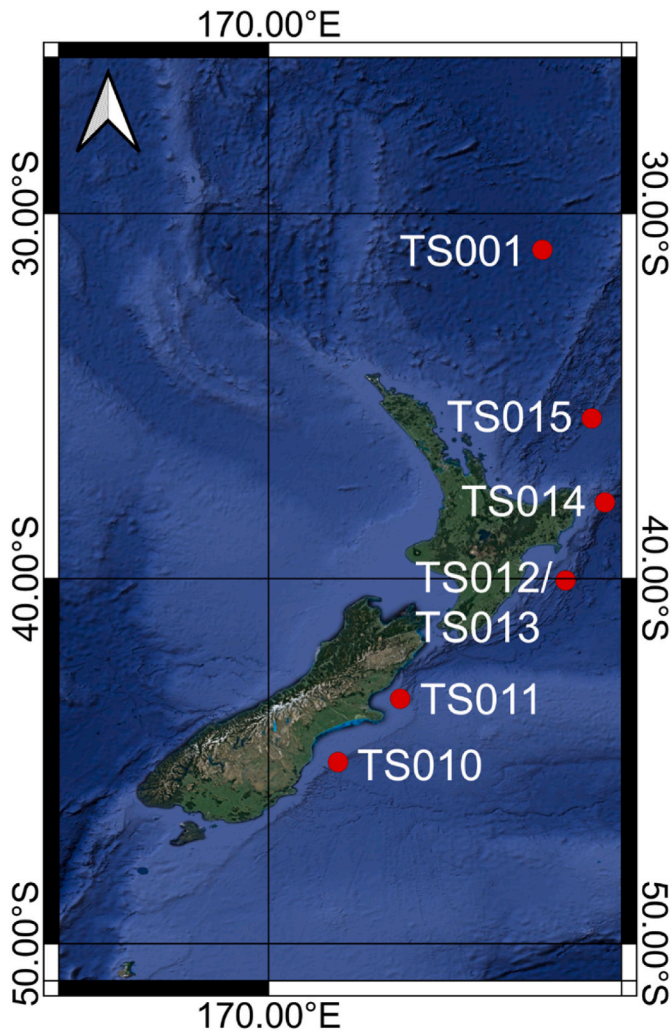
Fig. 1. Map with sampling sites (red dots) off New Zealand where the deep-sea sponges were collected for the incubations. Detailed information about species names and sampling depths are given in Table 1.

HydroFlash® O$_2$; Kongsberg Maritime Contros GmbH, Germany) which had been calibrated by 2-point calibration (0% calibration: Na$_2$SO$_3$; 100% calibration: air-bubbled seawater). A second CUBE was placed over bare sediment in close proximity and served as control/blank. This

CUBE took water samples automatically at the same time intervals as the sponge incubation CUBE and measured oxygen concentration continuously. At the end of the incubation, the sponge was collected by the ROV and returned to the vessel in a closed biobox. Aboard, the length *L*, width *W*, and height *H* of the sponge was measured with a ruler to the nearest 0.1 cm and a subsample of sponge tissue was taken with a scalpel, rinsed in sterile seawater, flash-frozen in liquid nitrogen and stored at −80 °C for microbial analysis. An additional tissue sample was taken for species identification before the remaining sponge was frozen at −21 °C. Water samples for nutrient analysis were filtered through 0.45 μm filters into 10 ml vials and stored frozen (−21 °C).

2.2. Ex-situ incubation experiment

During R/V *Sonne* cruise SO254 sponges were collected randomly at water depths between 595 m and 1467 m (Table 1) with ROV Kiel 6000. Aboard, individual sponges of the same putative species were incubated for 5 h in three closed incubation chambers (cylinder height:17 cm, diameter: 10 cm, volume: 1.26 L; Fig. 2) filled with a mix of deep water from the sampling location and surface water at *in-situ* temperature in the dark. A fourth incubation chamber filled with the same water mix served as control/blank. Before the start (T0) and at the end of the incubations (T5), duplicate water samples were taken from each incubation chamber for inorganic nutrient concentration, filtered (0.45 μm filters), and stored frozen (−21 °C). During the incubations, seawater air saturation (% O$_2$) was recorded continuously in 1 s intervals using an optical oxygen meter (FireStingO$_2$, PyroScience GmbH, Germany) after 2-point optode calibration. After completing the incubations, length *L*, width *W*, and height *H* of each sponge specimen were measured and tissue subsamples for microbial community analysis were taken from several specimens (Table S1) with a scalpel. These samples were rinsed in sterile seawater, flash-frozen in liquid nitrogen, and stored at −80 °C. The remaining sponge tissue was frozen at −21 °C after another tissue subsample was taken from one specimen per putative species for species identification.

The experimental design of both sets of experiments is presented in Fig. 3.

2.3. Sample processing

2.3.1. Species identification

One sponge specimen per putative species was identified by spicule analysis or, in case of *Lissodendoryx (Ectyodoryx)* sp. indet., based on still photo analysis (see Fig. 4). Voucher specimens are deposited in the NIWA Invertebrate Collection, Wellington, New Zealand. Additionally,
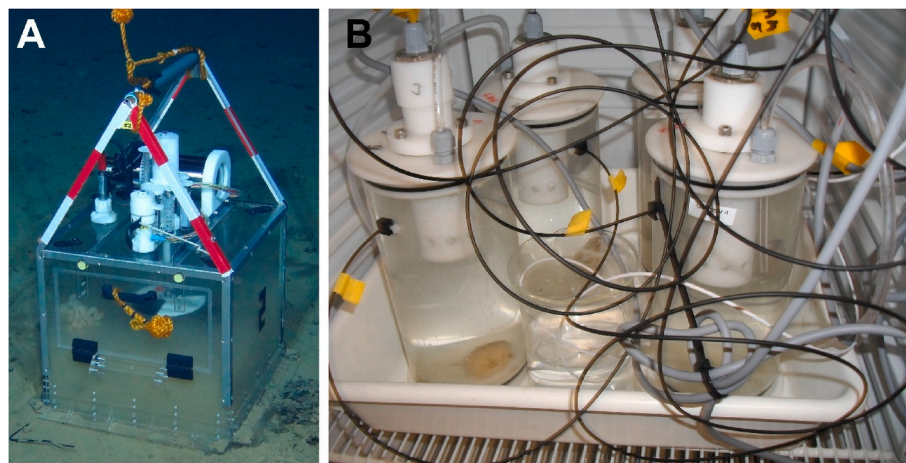

Fig. 2. Incubation of deep-sea sponges (A) *in-situ* at ∼4000 m water depth and (B) *ex-situ* aboard R/V Sonne. *In-situ* photo was taken with ROV Kiel 6000 (GEOMAR, Kiel, Germany) and *ex-situ* photo was taken by Tanja Stratmann.

small samples of sponge tissue were taken from each sponge specimen for DNA barcoding and matrix assisted laser desorption/ionization - time of flight mass spectrometry (MALDI-TOF MS).

For DNA-barcoding, sponge tissue was incubated in 30 µl Chelex (InstaGene™ Matrix, BioRad, USA) for 50 min at 56 °C and 10 min at 96 °C. In a total reaction volume of 20 µl, 2 µl DNA extract was mixed with 0.2 µl of forward (*16S1fw*) and reverse (*16SH_mod*) primers (Dohrmann et al., 2008), 10 µl Accu Start PCR mix (2 × PCR master mix, Quantabio, USA), and 7.6 µl molecular grade water. The PCR protocol was adapted from Kersken et al. (2018) using the following settings: initial denaturation for 5 min at 94 °C followed by 40 cycles of denaturation at 94 °C for 30 s, annealing for another 30 s at 48 °C, and elongation at 72 °C for 45 s. This was followed by a final elongation for 3 min at 72 °C. Sanger sequencing was carried out at Macrogen Europe (Amsterdam, Netherlands), producing chromatograms for forward and reverse sequences for each specimen. These chromatograms were processed in the *Geneious R7* software (version 7.0.6; https://www.geneious.com) to produce consensus sequences which were blasted (Altschul et al., 1997) to avoid contaminations. Final sequences were aligned in the *SeaView* software (Gouy et al., 2010) using the muscle algorithm and by-eye control. At the end, a neighbor joining analysis was carried out using Kimura two-parameter (K2P) distances to check for sequence similarities.

For MALDI-TOF MS, sponge tissue was incubated in a saturated solution of α-Cyano4-hydroxycinnamic acid (HCCA) dissolved in 50% acetonitrile, 47.5% molecular grade water, and 2.5% trifluoroacetic acid that completely covered the tissue as suggested by Rossel et al. (2024). After the incubation, 1.5 µl extract was transferred to a target plate and measured using a Microflex LT/SH System (Bruker Daltonics, USA). Molecule masses were measured from 2 to 20k Dalton (kDa) applying the *flexControl 3.4.* software (Bruker Daltonics). Peaks of a mass range between 2 and 20 kDa and a peak resolution of >400 were evaluated using the centroid peak detection algorithm with a signal-to-noise threshold of two and a minimum intensity threshold of 600. The proteins/oligonucleotide method was employed at a maximal resolution of 10 times above the threshold to validate fuzzy control. To create a sum spectrum, a total of 120 laser shots were applied to a spot which was measured three times each. Resulting mass spectra were processed with the *MALDIquantForeign* package (version 0.13) (Gibb, 2015) and the *MALDIquant* package (version 1.22) (Gibb and Strimmer, 2012) in *R* (version 4.2.2) (R-Core Team, 2022). Spectra were square-root transformed, smoothed using the Savitzky Golay method (Savitzky and Golay, 1964), baseline corrected using the SNIP method (Ryan et al., 1988), and spectra normalized using the total ion current (TIC) method. Repeated measurements were averaged using mean intensities. Peak picking was carried out using a signal to noise ratio (SNR) of 5 and a half window size of 17. Repeated peaks were binned to align homologous mass peaks. The resulting data were Hellinger transformed (Legendre and Gallagher, 2001) and hierarchically clustered in *R* using Ward's *D* and Euclidean distances.

Based on the DNA-barcoding and MALDI-TOF MS results (Supplementary Material; Fig. S2), sponges were classified in six sponge clusters (Fig. 3).

2.3.2. Sponge tissue analysis

Sponge volume (V, cm^3) was determined via water displacement (V_{WD}) and based on its geometric shape (V_{GS}). For the latter, each sponge was classified into different three-dimensional geometric shapes (cuboid, sphere, cylinder, circular cone, frustum; Fig. S3) and V_{GS} was calculated as:

$$V_{GS} \text{ for cuboid}: V_{GS} = L \times W \times H, \qquad \text{[Equation 1]}$$

$$V_{GS} \text{ for a sphere}: V_{GS} = \frac{4}{3}\pi R^2, \qquad \text{[Equation 2]}$$

$$V_{GS} \text{ for a cylinder}: V_{GS} = \pi \left(\frac{D}{2}\right)^2 \times H, \qquad \text{[Equation 3]}$$

$$V_{GS} \text{ for a circular cone}: V_{GS} = \frac{\pi \left(\frac{D}{2}\right)^2 \times H}{3}, \qquad \text{[Equation 4]}$$

$$V_{GS} \text{ for a Frustum}: V_{GS} = \frac{H \times \pi}{3} \times \left(R_2^2 + R_2 \times R_1 + R_2^2\right), \qquad \text{[Equation 5]}$$

where L = sponge length, W = sponge width, H = sponge height, R = sponge radius, D = diameter of the sponge, and R_1 and R_2 correspond to the two different radii in Fig. S3. The V_{GS}:V_{WD}-ratio for the different sponges species clusters is presented in Table S3.

Sponge wet mass (WM, g) of remaining tissue was measured with a balance to the nearest 0.001 g. Dry mass (DM, g) was determined after freeze-drying and ash-free dry mass ($AFDM$, g) was measured after oxidizing sub-samples (0.1 g) of freeze-dried sponges in a muffle furnace at 450 °C for 4 h. Total carbon (TC, % DM)/δ^{13}TC content and total nitrogen (TN, % DM)/δ^{15}N content of ~20 mg freeze-dried, finely-ground, homogenized sponge tissue samples were measured with a Thermo Flash EA 1112 elemental analyzer (EA; Thermo Fisher Scientific, USA) coupled to a DELTA V Advantage Isotope Ratio Mass Spectrometer (IRMS; Thermo Fisher Scientific, USA). To study organic carbon (org. C, % DM)/δ^{13}org. C content of the sponges, ~20 mg tissue powder was packed in 8 × 5 mm pre-combusted (4 h at 450 °C) silver capsules, acidified with 20 µL 2% HCl, and dried at 60 °C on a hot plate. Afterwards, capsules were closed and measured with the same EA-c-IRMS.

Total WM (g) and org. C (g) of each incubated sponge specimen was determined based on V_{GS} using the onboard size measurements of the sponges and conversion factors from Table S3, because no sponge arrived intact in the Netherlands due to the subsampling aboard.

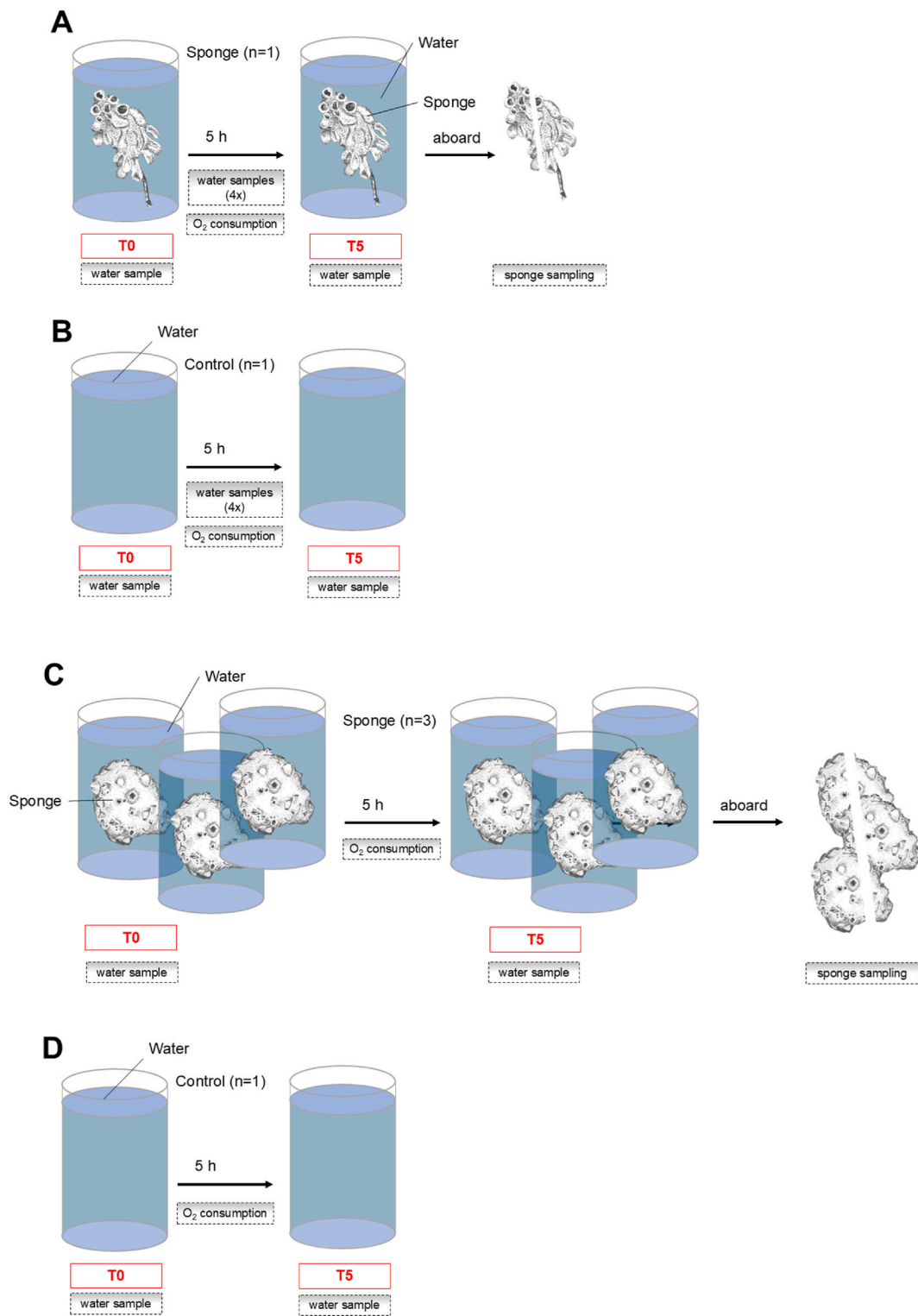Sponge condition index CI (−) was calculated following Lüskow et al. (2019):

Table 1
Detailed information about sampling location and species name of all collected sponges.

Sample ID	Geographical location	Latitude (°N)	Longitude (°E)	Depth (m)	T (°C)	Species [Class, Family]
TS001	Abyssal plain	−30.991	177.500	4160.9	1.5	*Saccocalyx tetractinus* (Reiswig and Kelly, 2018) [Hexactinellida, Euplectellidae]
TS010	Canterbury shelf slope	−45.026	171.904	646	6.0	*Suberites* spp. indet. [Demospongiae, Suberitidae]
TS011	Pegasus canyon. off Canterbury	−43.293	173.607	851.6	6.0	*Tedania* spp. indet. [Demospongiae, Tedaniidae]
TS012	Seamount # 986, off Hawke's Bay	−40.049	178.138	885	6.6	*Halichondria* sp. indet. [Demospongiae, Halichondriidae]
TS013	Seamount # 986, off Hawke's Bay	−40.045	178.142	856.9	6.0	*Dendoricella* spp. indet. [Demospongiae, Dendoricellidae]
TS014	Seamount # 1247, off East Cape	−37.913	179.214	1466.6	3.3	Sceptrulophora spp. indet. [Hexactinellida]
TS015-C1	Southern Kermadec Ridge	−35.612	178.852	1149.9	4.7	Sceptrulophora spp. indet. [Hexactinellida]
TS015-C2	Southern Kermadec Ridge	−35.611	178.852	1152.8	4.7	*Lissodendoryx (Ectyodoryx)* sp. indet. [Demospongiae, Coelosphaeridae]

Abbreviation: T = water temperature.

Fig. 3. Experimental design of the *in-situ* experiment (**A** sponge treatment, sample ID TS001; **B** control treatment) and the *ex-situ* experiment (**C** sponge treatment, sample IDs TS010 – TS014, TS015-C1, TS015-C2; **D** water treatment). Notice that for sampling IDs TS010 – TS014, a treatment consisted of 3 sponge incubations +1 control incubation. TS1015, however consisted of only 2 sponge incubations +1 control incubation.

$$CI = \frac{AFDM_V}{(DM_V - AFDM_V)},$$ [Equation 6]

where $AFDM_V$ is the volume specific ash-free dry mass (g ADFM cm^{-3} sponge) and DM_V is the volume specific dry mass (g DM cm^{-3} sponge).

2.3.3. Fatty acid extraction and analysis

PLFAs were extracted from ~100 mg freeze-dried, finely-ground, homogenized sponge tissue following a modified version of the Bligh and Dyer extraction method (Bligh and Dyer, 1959; de Kluijver, 2021; de Kluijver et al., 2021): Total lipids from sponge tissue were extracted in sampling tubes with 15 ml methanol (MeOH), 7.5 ml dichloromethane
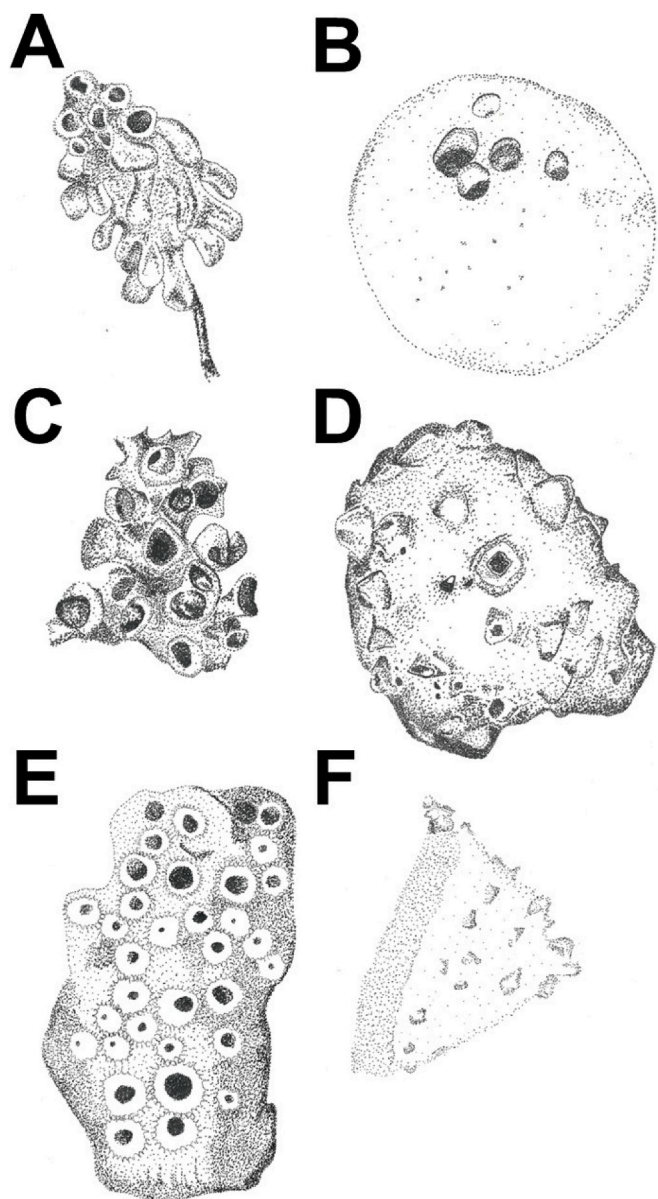
therefore collected and dried in the TurboVap evaporator.

Phospholipids were derivatized to fatty acid methyl esters (FAMEs) via mild alkaline methylation. For this, the dried sample was dissolved in 1 ml MeOH/toluene (1:1 v/v) and 1 ml 0.2 mol l^{-1} methanolic NaOH. 50 μL 0.1 mg ml^{-1} internal $C_{19:0}$-FAME standard was added and the whole solution was incubated for 15 min at 37 °C. The methylation was stopped by adding 2 ml hexane, 0.3 ml 1 mol l^{-1} acetic acid, and 2 ml Milli-Q water to the vial and shaking well. When the layers had separated, the hexane-containing upper layer was transferred to a new vial and this step was repeated twice before the hexane was evaporated until complete dryness. 50 μl 0.1 mg ml^{-1} internal $C_{12:0}$-FAME standard was added, 100 μl hexane was added and the solution was transferred to a GC analysis vial.

All samples were stored at −20 °C until FAMEs concentrations were measured on a gas chromatograph (GC) with flame ionization detector (FID) (HP 6890 series) on a non-polar analytical column (Agilent, CP-Sil5 CB; 25 m × 0.32 mm × 0.12 μm). The retention times of the individual peaks on the gas chromatogram were converted to equivalent chain length (ECL) using the retention times of the standard $C_{12:0}$-FAME, $C_{16:0}$-FAME, and $C_{19:0}$-FAME. The concentration of every individual FAMEs (μg g dry mass^{-1}) was quantified using the known concentration of $C_{12:0}$-FAME.

2.3.4. Analysis of bacterial communities of sponges

Ten sponge specimens from the incubation experiments were analyzed for their bacterial community composition (Table S1). DNA was extracted of ~0.25 g of sponge tissue and its quality and quantity were checked by NanoDrop and gel electrophoresis after a PCR with universal 16S rRNA gene primers. Then, the bacterial V3 to V4 variable regions were amplified in a one-step PCR, using the primer pair 341F-806R (Caporaso et al., 2011; Muyzer et al., 1993). Before sequencing the bacterial libraries on a MiSeq platform (MiSeqFGx, Illumina) with v3 chemistry, a quality check was performed by gel electrophoresis, normalization, and pooling.

Amplicon sequences were processed within QIIME2 (version 2019–10) (Bolyen et al., 2019). Demultiplexed forward reads were imported into QIIME2 and primers were trimmed. Amplicon sequence variants (ASVs) were generated from single-end reads (truncated to 270 nt) with the DADA2 algorithm (Callahan et al., 2016). Representative ASVs were taxonomically classified with the SILVA database (version 138 99% OTUs 16S) (Quast et al., 2013), using bacterial primer specific trained Naïve Bayes taxonomic classifiers.

2.3.5. Inorganic nutrient concentration measurements and flux calculations

Water samples for inorganic nutrient analysis were thawed for 24 h prior to the measurements of ammonium, nitrite, nitrate, and phosphate with a SEAL QuAAtro analyzer (Bran + Luebbe, Germany).

For the *ex-situ* incubations, blank- and biomass-corrected fluxes ($F_{i.nut}$) of the inorganic nutrients (μmol g C^{-1} d^{-1}) were calculated as follows:

$$F_{i.nut} = \frac{(i.nut_{sponge,T5} - i.nut_{blank,T5}) - (i.nut_{sponge,T0} - i.nut_{blank,T0})}{t \times tC\,content_{sponge}} \times (V_I - V_S),$$

[Equation 7]

where $i.nut_{sponge}$ is the inorganic nutrient concentration (μmol l^{-1}) in the incubation chamber with the sponge. $i.nut_{blank}$ is the inorganic nutrients concentration in the incubation chamber filled with seawater (*blank*). *T0* corresponds to the start of the incubation and *T5* corresponds to the end of the incubation after 5 h t is the incubation time (=0.21 d) and $tC\,content_{sponge}$ is the total org. C content of the incubated sponge (g C). V_I is the volume of the incubation chamber (=1.26 l) and V_S is the volume of the sponge (l).

For the *in-situ* incubation, fluxes ($F_{i.nut}$) of the inorganic nutrients (μmol g C^{-1} d^{-1}) were calculated as follows:

Fig. 4. Drawings of the six sponge clusters A) *Saccocalyx* cluster, B) *Suberites* cluster, C) Sceptrulophora cluster, D) *Tedania* cluster, E) *Halichondria/Dendoricella* cluster, F) *Lissodendoryx* cluster. Sizes of sponge clusters in the drawing are not to scale. Illustrations by Tanja Stratmann.

(DCM), and 6 ml phosphate (P)-buffer (8.7 g K_2HPO_4 dissolved in 1 l MilliQ-water, pH adjusted to 7–8 with 1 mol l^{-1} HCl) during constant shaking for 3 h. After addition of 7.5 ml DCM and 7.5 ml P-buffer, layers separated by leaving the sample tubes in the freezer (−21 °C) over night. The DCM layer was transferred to new tubes and 7.5 ml DCM were again added to the original tube. After the layers separated via centrifugation with 170 *g* for 3 min at room temperature, the DCM layer was transferred to the same new tube and evaporated to complete dryness in a TurboVap evaporator under gentle N_2-stream. 1 ml of DCM was added and evaporated again to complete dryness, before the sample was dissolved in 1 ml DCM:MeOH (1:1), transferred to a new vial, and dried at a FlexiVap™ Work Station under gentle N_2 stream.

To separate the Bligh and Dyer extract into the different polarity classes, the sample was dissolved in 0.5 ml DCM and added to a column with silica acid gel (activated at 120 °C for 2 h). Subsequently, the sample on the silica column was eluted with 7 ml acetone and 15 ml MeOH. The latter fraction contained the phospholipids and was

$$F_{i.nut} = \frac{(LR_{slope.sponge} - LR_{slope.blank}) \times (V_{CUBE} - V_S)}{tC\ content_{sponge}},$$ [Equation 8]

where $LR_{slope,\ sponge}$ and $LR_{slope,\ water}$ are the estimated slopes of the linear regression analyses performed with the concentrations of inorganic nutrients (μmol l^{-1}) collected over 5 h during the *in-situ* incubations as response (dependent) variable and time as predictor (independent) variable. $tC\ content_{sponge}$ is the total org. C content of the incubated sponge (g C). V_{CUBE} is the volume of the CUBE (=125 l) and V_S is the volume of the sponge (l).

A list with inorganic nutrient concentrations at the begin of the *in-situ* and *ex-situ* sponge incubation experiments is shown in Table S2.

2.3.6. Oxygen consumption calculations

Air saturations recorded by the oxygen meter in the *ex-situ* experiments were converted to absolute oxygen concentrations (μmol $O_2\ l^{-1}$) following (Weiss, 1970) using the *marelac* package (Soetaert et al., 2010) in *R*. Subsequently, average decrease in oxygen over time (ΔO_2, mmol $O_2\ l^{-1}\ d^{-1}$) in the *in-situ* and *ex-situ* experiments was calculated by linear regression and blank and biomass-corrected metabolic rate *R* (mmol O_2 g $C^{-1}\ d^{-1}$) was calculated as:

$$R = \frac{(\Delta O_{2.sponge} - \Delta O_{2.blank}) \times (V_I - V_S)}{tC\ content_{sponge}}.$$ [Equation 9]

2.4. Statistical analysis

We tested whether average inorganic nutrient and oxygen fluxes of the same sponge cluster differed significantly from 0 μmol g $C^{-1}\ d^{-1}$ using a 1-sided Student's t-test ($\alpha = 0.05$) in *R* (version 4.3.0) after normality of data was confirmed with a Shapiro-Wilk normality test. When data were not normally distributed, a 1-sample Wilcoxon test ($\alpha = 0.05$) was performed in *R*.

Statistical differences in microbial community composition between the *Halichondria/Dendoricella* cluster, the *Tedania* cluster, and the Sceptrulophora cluster were investigated by pairwise PERMANOVAs and nonmetric multidimensional scaling (nMDS) using the R package *vegan* (Oksanen et al., 2017). The microbial community composition of the *Lissodendoryx* cluster, the *Suberites* cluster, and the *Saccocalyx* cluster were not assessed statistically, because this parameter was studied in n < 2 specimens per cluster.

Statistical difference in TC of sponge tissue between the *Halichondria/Dendoricella* cluster and the Sceptrulophora cluster was assessed by the non-parametric Kruskal-Wallis rank sum test *H* ($\alpha = 0.05$), after the Bartlett test of homogeneity of variances ($\alpha = 0.05$) revealed that the variances of the two clusters was different. Differences in org. C, TN, δ^{13}org. C, δ^{13}TC, and δ^{15}N of the two sponge clusters were assessed by 1-Way ANOVA, as the Bartlett test of homogeneity of variances ($\alpha = 0.05$) confirmed homogeneity of variances.

All data are presented as mean $\pm$ standard error.

3. Results

3.1. (Biochemical) composition of sponge tissue

Sponges consisted of 82.4 $\pm$ 3.91% water (n = 18) and their dried tissue contained 5.47 $\pm$ 0.75% TC, 4.47 $\pm$ 0.52% org. C, and 1.06 $\pm$ 0.15% TN (n = 15). The *Halichondria/Dendoricella* cluster (n = 5) had the lowest TC (3.25 $\pm$ 0.35%), org. C (2.86 $\pm$ 0.39%), and TN contents (0.65 $\pm$ 0.08%), whereas the *Tedania* cluster (n = 2) had the highest TC (9.21 $\pm$ 2.19%), org. C (7.17 $\pm$ 0.31%), and TN contents (1.87 $\pm$ 0.43%). Sponge *CI* ranged from 0.11 $\pm$ 0.02 for the *Tedania* cluster (n = 3) to 0.34 $\pm$ 0.00 for the *Suberites* cluster (n = 3). The mean δ^{13}org. C-value of the sponges was -17.6 ± 0.57‰ [min: -20.1 ± 0.35‰, Sceptrulophora cluster, n = 4; max: -14.1‰, *Saccocalyx* cluster, n = 1), the mean δ^{13}TC-value was -19.0 ± 0.28‰ [min: -20.3 ± 0.09‰,

Sceptrulophora cluster, n = 4; max: -17.0 ± 0.24‰, *Tedania* cluster, n = 2), and the mean δ^{15}N-value was 18.5 $\pm$ 1.28‰ [min: 10.2‰, *Lissodendoryx* cluster, n = 1; max: 23.5‰, *Saccocalyx* cluster, n = 1) (Fig. 5).

When comparing the biochemical composition of sponges from the *Halichondria/Dendoricella* cluster with the Sceptrulophora cluster, TC, δ^{13}TC, δ^{13}org. C, and δ^{15}N of the sponge tissue differed significantly between clusters (Table 2).

3.2. Nutrient fluxes and oxygen consumption

All sponges released nitrite and ammonium (Fig. 6), but only the nitrite release of the *Halichondria/Dendoricella* cluster (1.45 $\pm$ 0.35 μmol g $C^{-1}\ d^{-1}$) and the *Suberites* cluster (2.17 $\pm$ 0.44 μmol g $C^{-1}\ d^{-1}$) and the ammonium release of the *Tedania* cluster (2.25 $\pm$ 0.55 μmol g $C^{-1}\ d^{-1}$) and the *Halichondria/Dendoricella* cluster (90.7 $\pm$ 22.8 μmol g $C^{-1}\ d^{-1}$) were significantly different from 0 μmol g $C^{-1}\ d^{-1}$; though, no statistical analyses of nutrient and oxygen fluxes were performed for the *Saccocalyx* cluster and the *Lissodendoryx* cluster (Fig. 6; Table 3). Nitrate was released by the *Halichondria/Dendoricella* cluster and the *Lissodendoryx* cluster, and consumed by the *Suberites* cluster, the *Tedania* cluster, and the Sceptrulophora cluster, though all statistically tested fluxes were not significantly different from 0 μmol g $C^{-1}\ d^{-1}$ (Fig. 6; Table 3). Phosphate release was only significantly different from 0 μmol g $C^{-1}\ d^{-1}$ in the case of the Sceptrulophora cluster (2.10 $\pm$ 0.47 μmol g $C^{-1}\ d^{-1}$) and the *Halichondria/Dendoricella* cluster (18.5 $\pm$ 4.83 μmol g $C^{-1}\ d^{-1}$) (Fig. 6; Table 3).

Sponges consumed between 0.17 mmol O_2 g $C^{-1}\ d^{-1}$ (*Saccocalyx* cluster) and 3.56 $\pm$ 0.60 mmol O_2 g $C^{-1}\ d^{-1}$ (*Suberites* cluster) oxygen (Fig. 6), but the oxygen consumption rate of the *Tedania* cluster was not significantly different from 0 mmol O_2 g $C^{-1}\ d^{-1}$ (Table 3). Oxygen fluxes
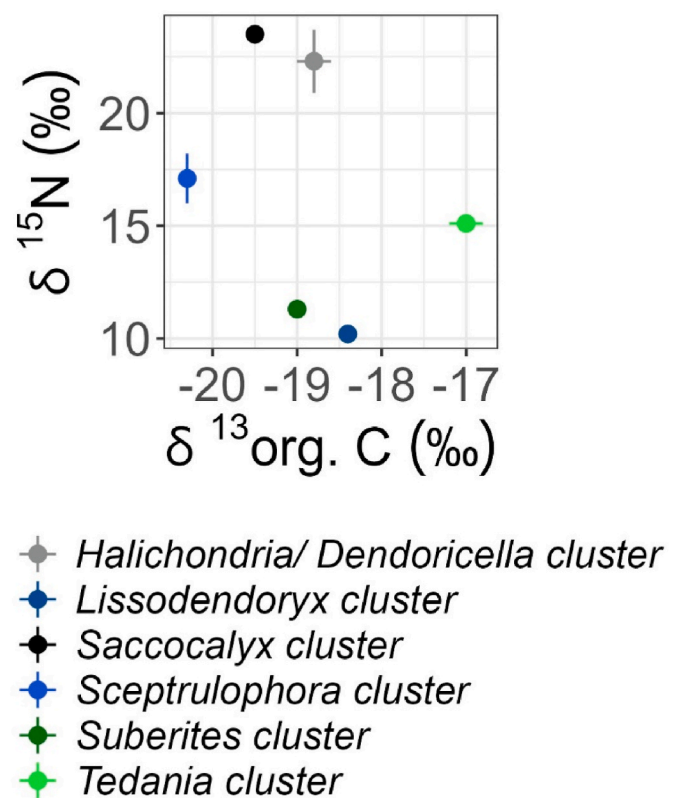

Fig. 5. Isotopic composition of carbon (δ^{13}org. C, ‰) and nitrogen (δ^{15}N, ‰) of sponge tissue collected from New Zealand. Error bars represent 1 standard error; invisible error bars does not imply no standard error was plotted, but instead it indicates that the plotted standard error was very small and therefore not visible in the plot.

Table 2

Results of 1-Way ANOVA to compare the biochemical composition of sponge tissue of the *Halichondria/Dendoricella* cluster with the Sceptrulophora cluster. Symbols: *p-value$\leq$0.05, ‡p-value$\leq$0.01

Parameter	df	F-value	H	p-value
TC	1		6.54	0.011*
org. C	1	7.79		0.024
TN	1	3.37		0.104
δ^{13}TC	1	10.15		0.013*
δ^{13}org. C	1	28.62		0.001‡
δ^{15}N	1	6.828		0.031*

presented per sponge volume, sponge wet/dry/ash-free dry mass are presented in Table S4.

3.3. Fatty acid composition of sponges

The PLFA compositions (Fig. 7A and B; Table S5) differed among sponge clusters. Between 24.2% (*Halichondria/Dendoricella* cluster) and 59.4 % (*Saccocalyx* cluster) of the PLFAs found in sponges consisted of long-chain fatty acids (LCFA, i.e., fatty acid with $\geq$24 C atoms) (Fig. 7A). The other PLFA classes detected in sponges were branched fatty acids (0.84 $\pm$ 0.57%), cyclic fatty acids (2.36 $\pm$ 1.67%), highly unsaturated fatty acids (HUFA, i.e., fatty acids with $\geq$ 4 double bonds; 3.61 $\pm$
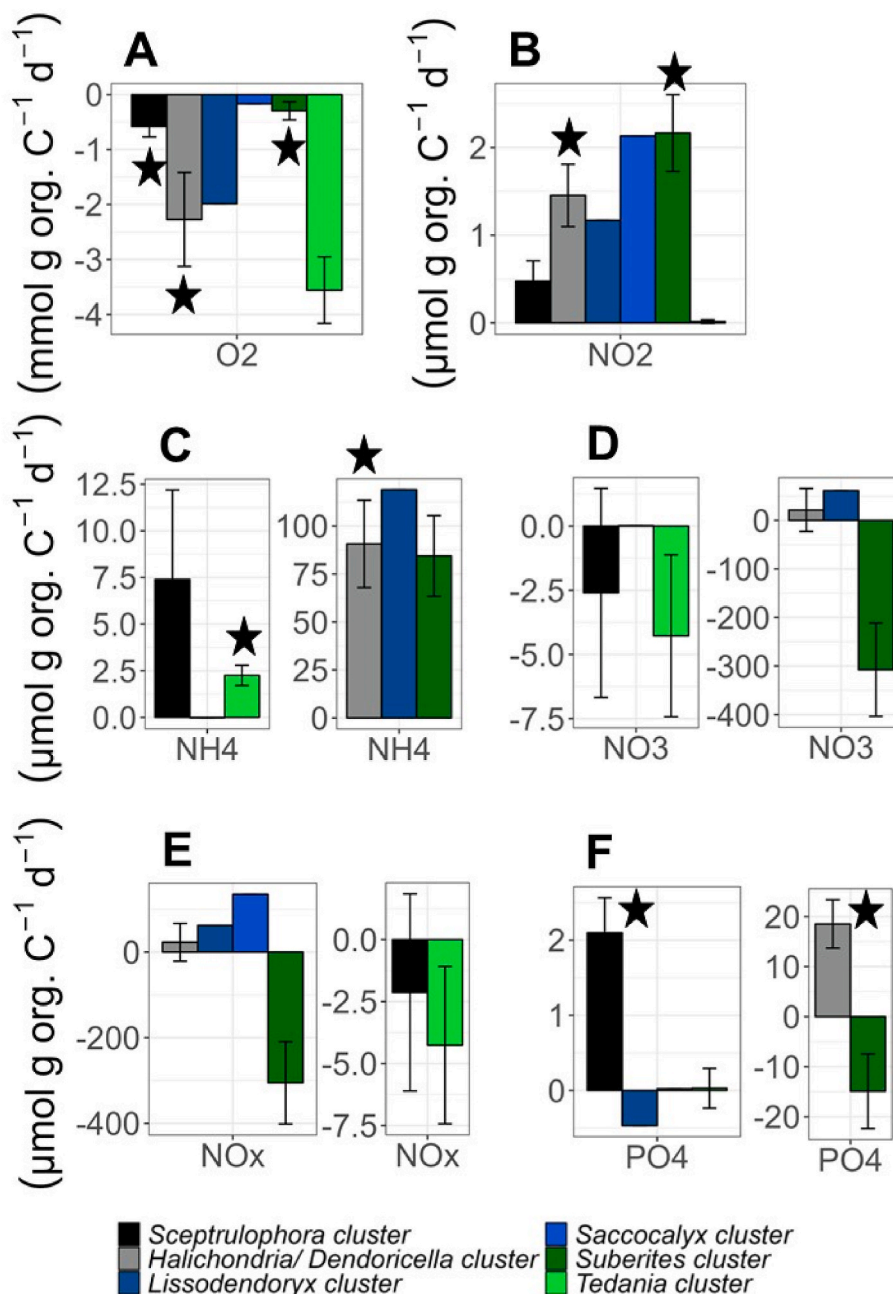

Fig. 6. Fluxes (mean $\pm$ 1 standard error) of (A) oxygen (O_2; mmol O_2 g org. C^1 d^{-1}), (B) nitrite (NO_2^-), (C) ammonium (NH_4^+), (D) nitrate (NO_3^-), (E) NO_x^- (i.e., nitrate + nitrite), and (F) phosphate (PO_4^{3-}) (all μmol g org. C sponge^{-1} d^{-1}). Negative fluxes signify that the sponges took up a specific compound, whereas positive fluxes mean that sponges released this compound. A star symbolizes that the average of this specific flux is significantly different from 0. No statistical analyses were performed for fluxes of the *Saccocalyx* cluster and the *Lissodendoryx* cluster, because only single sponges of these clusters were incubated. A table with nutrient fluxes calculated per sponge volume (cm^3), sponge wet mass (g *WM*), sponge dry mass (g *DM*), and sponge ash-free dry mass (g *AFDM*) is presented in Table S4.

Table 3

Results of 1-sided Student's t-tests (α = 0.05) and 1-sample Wilcoxon tests (α = 0.05) to assess whether oxygen consumption rates (mmol O_2 g org. C sponge^1 d^{-1}) and nutrient fluxes (μmol g org. C sponge^{-1} d^{-1}) were significantly different from 0 (H_0: μ = 0, H_1: μ ≠ 0). Symbols: *p-value≤0.05, ‡p-value≤0.01

| Sample ID	Flux type	df	t-value	V	Mean	95% Confidence interval	p-value
Sceptrulophora clustercluster (n = 4)	O_2	3	−3.06		−0.58	−1.18, −0.02	0.05*
	NH_4^+	3	1.54		7.39	−7.87, 22.7	0.22
	NO_2^-	3	2.05		0.48	−0.26, 1.21	0.13
	NO_3^-			6			0.88
	NO_x			6			0.88
	PO_4^{3-}	3	4.50		2.10	0.61, 3.58	0.02*
Halichondria/Dendoricella cluster (n = 6)	O_2	5	−2.66		−2.27	−4.47, −0.08	0.04*
	NH_4^+	5	3.98		90.7	32.1, 149	0.01‡
	NO_2^-	5	4.10		1.45	0.54, 2.37	0.009‡
	NO_3^-	5	0.49		21.5	−92.0, 135	0.65
	NO_x	5	0.52		22.9	−91.0, 137	0.63
	PO_4^{3-}	5	3.84		18.5	6.11, 30.9	0.01‡
Suberites cluster (n = 3)	O_2	2	−5.88		−3.56	−6.16, −0.96	0.03*
	NH_4^+	2	4.02		84.4	−6.03, 175	0.06
	NO_2^-	2	4.93		2.17	0.28, 4.05	0.04*
	NO_3^-	2	−3.20		−308	−721, 105	0.09
	NO_x	2	−3.18		−305	−718, 108	0.09
	PO_4^{3-}	2	−2.00		−14.9	−47.0, 17.2	0.18
Tedania cluster (n = 3)	O_2	2	−1.82		−0.30	−1.00, 0.41	0.21
	NH_4^+	2	4.12		2.25	−0.10, 4.60	0.05*
	NO_2^-	2	0.72		0.01	−0.07, 0.10	0.55
	NO_3^-	2	−1.35		−4.27	−17.8, 9.30	0.31
	NO_x	2	−1.34		−4.26	−17.9, 9.39	0.31
	PO_4^{3-}	2	0.11		0.03	−1.11, 1.17	0.92
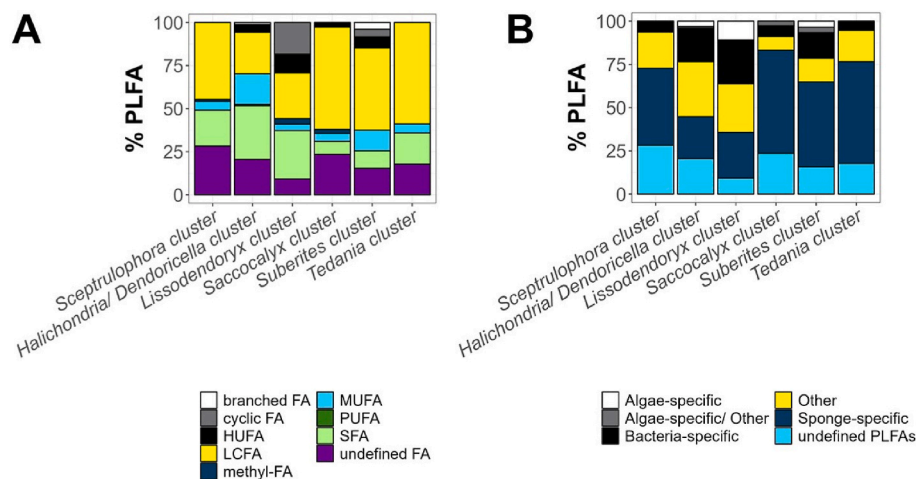
Fig. 7. (**A**) Contribution (%) of individual phospholipid-derived fatty acid (PLFA) classes to the total concentrations in sponges. (**B**) Contribution (%) of individual PLFA categories to total PLFA concentrations in sponges.
Abbreviations: branched FA = branched fatty acid, HUFA = highly unsaturated fatty acid, LCFA = long-chain fatty acid, methyl-FA = methyl-fatty acid, MUFA = monounsaturated fatty acid, PUFA = polyunsaturated fatty acid, SFA = saturated fatty acid.

1.50%), methyl-fatty acids (0.73 ± 0.38%), monosaturated fatty acids (MUFA; 11.3 ± 2.14%), polyunsaturated fatty acids (PUFAs, i.e., fatty acids with ≥2 double bonds; 0.35 ± 0.35%), saturated fatty acids (SFA; 23.8 ± 2.77%), and undefined fatty acids (20.4 ± 3.03%).

The highest concentrations of PLFAs isolated from the sponge tissue were sponge-specific PLFAs (min: 24.2% of total PLFA concentration, *Halichondria/Dendoricella* cluster; max: 59.7%, *Saccocalyx* cluster) (Fig. 7B). The PLFA categories with the second and third highest concentrations consisted of others (min: 7.95% *Saccocalyx* cluster; max: 31.9% *Halichondria/Dendoricella* cluster) and bacteria-specific PLFAs (min: 5.25%, *Tedania* cluster; max: 25.3%, *Lissodendoryx* cluster). About 9.21% (*Lissodendoryx* cluster) to 28.2% (Sceptrulophora cluster) of the total PLFA concentration consisted of undefined PLFAs.

3.4. Composition of sponge-associated bacterial community

The bacterial community in all sponge clusters, except for the *Suberites* cluster, were dominated by Proteobacteria (min: 84.8 ± 5.58% ASVs *Tedania* cluster; max: 95.3 ± 0.82% ASVs *Halichondria/Dendoricella* cluster), followed by Bacteroidota (0.28 ± 0.01% − 5.50 ± 2.67% ASVs), Planctomycetota (0.26 ± 0.08% − 1.11 ± 0.44% ASVs), and Nitrospinota (0.03 ± 0.02% − 3.34 ± 1.74% ASVs) (Fig. 8, Table S6). The most abundant Bacteria in the *Suberites* cluster were Proteobacteria (44.3% ASVs), Chloroflexota (20.3% ASVs), Acidobacteriota (13.7% ASVs), and Actinobacteriota (3.10% ASVs) (Fig. 8).

Statistical comparisons revealed no significant differences in bacterial community composition between the Sceptrulophora cluster, *Tedania* cluster, or *Halichondria/Dendoricella* cluster (Table 4, Fig. 9).

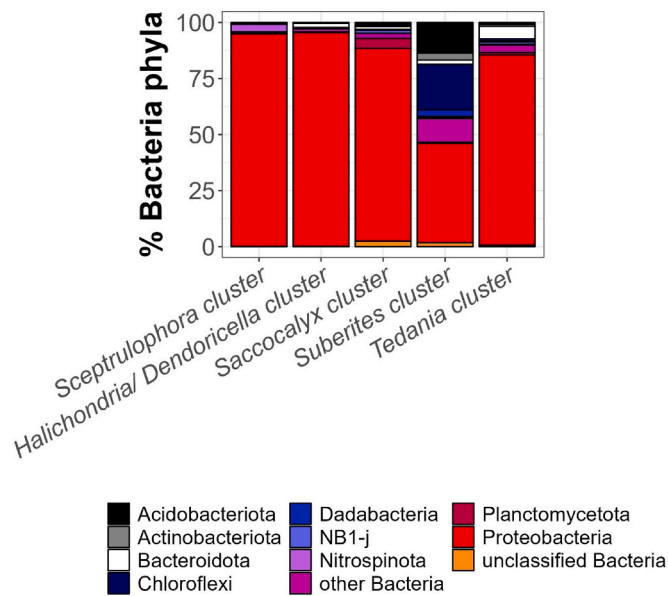**Fig. 8.** Relative abundance of bacteria phyla (%) in the five analyzed sponge clusters. The nine most abundant microbial phyla are indicated by names, others are aggregated under the category "other Bacteria" and "unclassified Bacteria".

Table 4

Results of pairwise PERMANOVAs to assess statistical differences in bacterial community composition between sponge clusters.

Comparisons	Sample size n	pseudo-F	p-value
Sceptrulophora cluster vs. *Tedania* cluster	5	14.46	0.095
Sceptrulophora cluster vs. *Halichondria/ Dendoricella* cluster	6	67.66	0.103
Tedania cluster vs. *Halichondria/Dendoricella* cluster	5	31.06	0.100

Fig. 9. Nonmetric multidimensional scaling (nMDS) plot of the bacterial community composition of the different sponge clusters.

4. Discussion

Here, we measured inorganic nutrient fluxes and oxygen consumption in deep-sea sponges collected randomly during an exploratory research expedition around New Zealand which aimed at better understanding the underwater biodiversity in the temperate Australasia biogeographic realm. We furthermore tried to link results from flux measurements with the fatty acid composition of sponges and the microbial communities associated with different sponge clusters.

4.1. Study limitations

As deep-sea science is logistically challenging and very expensive, this study had several shortcomings in its methodological approach. The biggest limitation was the reduced number of replicates to study the biochemical composition of sponge tissue, and the microbial and PLFA composition. This was related to post-cruise subsampling when several specimens were selected for additional analyses of their marine natural products. Additionally, subsamples for DNA barcoding and sponge spicules should have been taken from each specimen and not only once per incubation treatment to confirm putative species identification. In this way, clustering of several species would have been obsolete.

To assess how the incubation changed the sponge microbiome, additional sponge specimens should have been collected in the field and immediately subsampled for further microbial analyses. These results could be compared with the microbiome of sponge specimens that were previously incubated to assess potential effects of the incubations on the
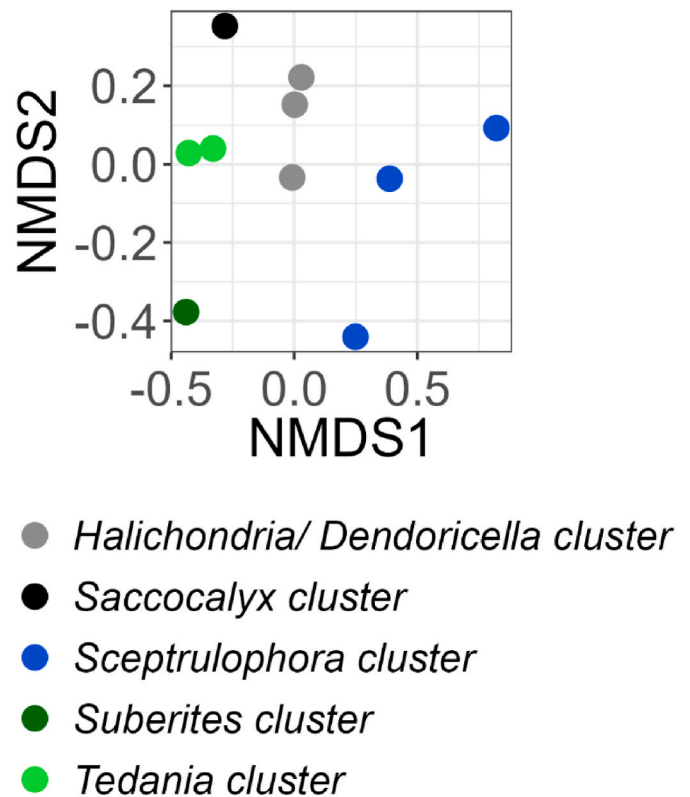
sponge microbiome.

Furthermore, previous work with deep-sea hexactinellid sponges incubated in water originated from shallower water depth revealed that sponges that consume ammonium *in situ* started to release ammonium *ex situ* (Maldonado et al., 2021). This effect could be related to rapid changes in the microbial community composition of the sponges when they were exposed to shallow seawater which might have triggered a change in the holobiont metabolism and therefore changed the direction and magnitude of the nutrient fluxes. Therefore, deep-sea sponges should always be incubated in seawater originating from their natural habitat to impede alterations of their microbiome and shifts in the metabolic pathways.

4.2. Nitrogen fluxes of deep-sea sponges

The dissolved inorganic nitrogen (DIN) dynamics of the sponge clusters collected from New Zealand comprised the uptake of nitrate and the release of ammonium, nitrate, and nitrite. Most ammonium was excreted by the *Lissodendoryx* cluster, whereas most NO_x^- (i.e., nitrate + nitrite) release was detected in the *Suberites* cluster. A high excretion of NO_x^- by the HMA sponge *Suberites* spp. indet. is not uncommon and has been observed in other studies of HMA sponges from Florida Bay (W Atlantic) (Hoer et al., 2018; Southwell et al., 2008), whereas LMA sponges, such as all other sponge clusters investigated in this study, predominantly excrete ammonium (Hoer et al., 2018).

A more detailed look at the DIN fluxes measured *ex situ* and *in situ* revealed three different types of nitrogen cycling in sponges. Type 1 is represented by the release of ammonium and NO_x^- by *Dendoricella* spp. indet. and the *Lissodendoryx* cluster (Fig. S4). Type 2 is the release of ammonium and the uptake of NO_x^- by the Sceptrulophora cluster, *Halichondria* sp. indet., the *Suberites* cluster, and the *Tedania* cluster and type 3 comprises a minimal release of ammonium and the release of NO_x^- by the *Saccocalyx* cluster.

During type 1, the sponge holobiont aerobically respires and ammonificates organic matter to ammonium, fixes N_2 to ammonium (likely a minor process), and aerobically nitrifies part of the heterotrophically produced ammonium to nitrate and nitrite. This type of N cycling is not limited to the investigated deep-sea sponges from New Zealand, but has also been observed in the shallow-water sponges *Ircinia felix* (Duchassaing de Fonbressin and Michelotti, 1864), *Ircinia campana* (Lamarck, 1814), and *Dasycladus* sp. (previously *Spongia* sp.) from Florida Bay and *Xestospongia muta* (Schmidt, 1870) from the Caribbean (Fiore et al., 2013; Hoer et al., 2018). In the investigated sponges from New Zealand, however, the dominating N cycling processes might vary as the $\delta^{15}N$ values of sponge tissue differ substantially between *Dendoricella* spp. indet. and the *Lissodendoryx* cluster. The very high $\delta^{15}N$ *Dendoricella* spp. indet. tissue value (23.8 ± 2.36‰) resembles nitrification which is believed to lead to a net enrichment in $\delta^{15}N$ of sponge tissue (Southwell, 2007). In comparison, the lower $\delta^{15}N$ *Lissodendoryx* cluster tissue value (10.2‰) indicates that this cluster nitrifies, but also likely feeds more selectively than *Dendoricella* spp. indet. and/or takes up more dissolved organic matter (DOM) and/or fixes more N_2 than *Dendoricella* spp. indet. (Southwell, 2007). Unfortunately, we did not take samples for bacterioplankton, DOM or dissolved N_2 concentrations to verify these hypotheses.

During type 2, the sponge holobiont aerobically respires and ammonificates organic matter to ammonium and reduces nitrate anaerobically to ammonium via dissimilatory nitrate reduction to ammonium (DNRA). Dissimilatory nitrate reduction to ammonium requires anaerobic niches or 'pockets' within the sponge holobiont and, indeed, Kumala et al. (2021) measured oxygen gradients inside the temperate shallow-water sponge *Halichondria (Halichondria) panicea* (Pallas, 1766) and Gatti et al. (2002) detected differences in oxygen saturation inside sponge tissue of the Antarctic sponge *Suberites domuncula* (Olivi, 1792). In these anaerobic niches, DNRA is driven by the microbiome of the sponge holobiont, such as Planctomycetota and Actinobacteriota that are involved in DNRA in the deep-sea sponge *Vazella pourtalesii* (Schmidt, 1870) from Emerald Basin (NW Atlantic) (Maldonado et al., 2021).

Type 3 likely resembles the microbial nitrification of ammonium to nitrite and subsequently to nitrate by ammonium-oxidizing Bacteria (AOB) and/or Archaea (AOA) (Hallam et al., 2006; Hentschel et al., 2006; Preston et al., 1996; Steinert et al., 2020). *Nodastrella nodastrella* (Topsent, 1915) from Rockall Bank (NE Atlantic) and *V. pourtalesii* from Emerald Basin take up ammonium (Maldonado et al., 2021; Van Duyl et al., 2008) and mostly release nitrite instead of nitrate indicating that a subsequent oxidation of nitrite to nitrate does not happen within the sponge holobiont, potentially due to a lack of nitrite oxidizing bacteria (NOB) (Maldonado et al., 2021). Here, the *Saccocalyx* cluster releases very low amounts of ammonia suggesting that the microbial nitrification cycle is not completely closed and parts of the ammonium escape nitrification.

4.3. Bacterial community of the sponge holobionts

Microbial fingerprints indicated that all sponge clusters, except the *Suberites* cluster, were likely LMA sponges, being dominated by Proteobacteria. The *Suberites* cluster, however, was likely a HMA sponge, indicated among others by a large fraction of Chloroflexota bacteria and Acidobacteriota, besides Proteobacteria. Overall, the investigated sponges hosted microbiomes whose bacterial composition was comparable to other deep-sea sponges (Acidobacteriota, Chloroflexota, and Dadabacteria enriched in HMA over LMA sponges; Bacteroidota and Proteobacteria enriched in LMA over HMA), and resembled similar patterns as described in another study on deep-sea sponges from the same research cruise around New Zealand (Steinert et al., 2020).

In *V. pourtalesii* Proteobacteria are involved in the assimilation of ammonium, ammonification, and DOM processing and some Proteobacteria species contain the enzyme ammonia-monooxygenase (AMO)

which is responsible for the oxidation of ammonium to hydroxylamine, the first step of the nitrification (Maldonado et al., 2021). Hence, Proteobacteria present in *Dendoricella* spp. indet. and *Lissodendoryx* cluster might be involved in the ammonification of DOM. These bacteria could also participate in denitrification as clusters of Beta- and Gammaproteobacteria detected in *G. barretti* have the gene *nirS* encoding for the enzyme cytochrome cd1-containing nitrite reductase (Hoffmann et al., 2009). However, as we neither measured nitric oxide, not did we perform metatranscriptomics of the microbiome in our sponge clusters, we cannot confirm this.

Bacteroidota play a key role in tropical coral reefs, where they are involved in amino acid metabolism and biosynthesis of terpenoids and polyketides in seawater (Glasl et al., 2020). They can contain *SusD*-like genes and genes encoding for glycoside hydrolase pointing towards the ability of degrading polysaccharides (Glasl et al., 2020; Mackenzie et al., 2012). Indeed, Bacteroidota present in the shallow-water coral reef sponges *Ircinia ramosa* (Keller, 1889), *Ircinia microconulosa* Pulitzer-Finali, 1982 and *Phyllospongia foliascens* (Pallas, 1766) are involved in carbohydrate degradation (O'Brien et al., 2023). Also in *V. pourtalesii*, they contribute to DOM processing (Maldonado et al., 2021). Hence, Bacteroidota enriched in the *Tedania* cluster compared to other sponge clusters investigated here might be involved in the degradation of carbohydrates and ammonification of DOM which was measured as ammonium release.

Planctomycetota are involved in the nitrogen cycle of the sponge holobiont. In fact, metatranscriptomics of *V. pourtalesii* showed that members of this bacteria phylum have genes encoding for nitrate reductase which is necessary for the denitrification of nitrate to nitrite (Maldonado et al., 2021). Furthermore, they contain the genes *nirB/D* that encode for NADH dependent nitrate reductase that is part of the DNRA pathway and they accommodate genes for nitrogenase enzymes required for N_2 fixation to ammonium (Maldonado et al., 2021, 2024). In this study, however, Planctomycetota were most abundant in the *Saccocalyx* cluster where inorganic nutrient flux data indicate that neither DNRA nor denitrification happened at higher rates. We therefore expect that Archaea which were not investigated in this study might have been more active in nitrogen cycling of the *Saccocalyx* cluster than Planctomycetota.

Members of the phylum Nitrospinota are NOB that oxidize nitrite to nitrate and play an important role in dark carbon fixation (Pachiadaki et al., 2017) and nitrite oxidation in oxygen minimum zones (Sun et al., 2019). These bacteria are present in the shallow-water sponges *I. ramosa* and *Coscinoderma mathewsi* (Lendenfeld, 1886) (Australian Great Barrier Reef (Engelberts et al., 2020; Glasl et al., 2020), *Petrosia (Petrosia) ficiformis* (Poiret, 1789) (Eastern Mediterranean Sea (Burgsdorf et al., 2022);), and *Aplysina aerophoba* (Nardo, 1833) (Adriatic Sea (Burgsdorf et al., 2022);). In this study, they were most abundant in the *Farrea* cluster (3.34 ± 1.74% ASVs, Table S7), but as we measured (not significant) release of nitrite instead of uptake (Fig. 6), Nitrospinota were likely not very active in this sponge cluster.

Chloroflexota, which was the second most abundant bacteria phylum in the *Suberites* cluster, often dominate the bacterial community of HMA sponge holobionts (Bayer et al., 2018; Busch et al., 2020; Moitinho-Silva et al., 2017). Members of this phylum are aerobic heterotrophs that potentially perform autotrophic carbon fixation in parts of the sponge tissue that becomes anoxic when the sponge pumping activity ceases (Bayer et al., 2018). They also contain genes for fatty acid biosynthesis and degradation (Bayer et al., 2018). Two Chloroflexota classes (i.e., *Anaerolineae* and *Caldilineae*), in particular, are capable of extensive uptake of carbohydrates and their subsequent degradation (Bayer et al., 2018) and it has been speculated that Chloroflexota bacteria are even able to degrade recalcitrant DOM (Bayer et al., 2018; Landry et al., 2017). Hence, we hypothesize that the *Suberites* cluster might take up DOM, though we did not measure DOM fluxes in the incubations and therefore cannot confirm this hypothesis.

4.4. Fatty acid composition of deep-sea sponges

Knowledge about differences in (phospholipid-derived) fatty acid profiles of demosponges compared to glass sponges is still very limited, but the data available so far indicate that demosponges synthesize mainly dienoic long-chain fatty acids with 24–28 C-atoms, whereas glass sponges have long-chain fatty acids with mostly C30-polyunsaturated fatty acids (Thiel et al., 2002). Furthermore, demosponges contain methyl-branched carbon chains that are less common in glass sponges and brominated long-chain fatty acids which have not been observed in glass sponges (Garson et al., 1994; Thiel et al., 2002). The fatty acid composition of the sponges that were investigated here mostly confirm the previous observations: The concentration of long-chain fatty acids with 24–27 C-atoms was higher in demosponges than in glass sponges (Fig. S5). Fatty acids with 28–30 C-atoms, however, had higher concentrations in glass sponges than in demosponges (Fig. S5).

A closer look at the fatty acid composition of the different sponge clusters may provide additional information about food sources of these sponges. The presence of mid-chain branched fatty acids (8/9/10/11-Me-C16:0, 9/10/11-Me-C18) that are bacteria-originating precursor fatty acids for long-chain fatty acids (de Kluijver et al., 2021) show that the deep-sea sponge clusters *Farrea*, *Saccocalyx*, and *Lissodendoryx* gain metabolic energy from their endosymbionts, similar to what has been described for Geodiidae sponges from the Northeast Atlantic (de Kluijver et al., 2021).

The presence of algae-specific fatty acids in the *Lissodendoryx* cluster, the *Halichondria/Dendoricella* cluster and the *Suberites* cluster suggests that these sponges take up phytodetritus-derived POC. The results of the DIN flux measurements of the *Lissodendoryx* cluster and the *Suberites* cluster are evidence for this suggestion because both sponge clusters likely ammonificate organic matter. However, the algae-specific fatty acid C20:5ω3 (eicosapentaenoic acid *EPA*) can also be synthesized by deep-water corals, like *Desmophyllum pertusum* (Linnaeus, 1758) (Mueller et al., 2014). Hence, the presence of *EPA* which co-eluted with C20:4ω6 (α-linolenic acid *ARA*) indicates that the *Saccocalyx* cluster, the *Halichondria/Dendoricella* cluster, and the *Suberites* cluster might also consume DOM originating from the mucus of deep-water corals. In fact, ROV imagery from the sampling stations show the presence of deep-water corals in the vicinity of the *Suberites* cluster (Fig. S6).

5. Conclusions

In this study, we assessed the role of deep-sea sponge holobionts from New Zealand in nitrogen cycling and tried to decipher the potential food-source preferences of these sponges. Sponges of the LMA Sceptrulophora cluster potentially gain metabolic energy from their symbionts and host AOB that might oxidize ammonia to nitrite. Members of the LMA *Saccocalyx* cluster might gain metabolic energy from endosymbionts, such as Proteobacteria, and might host bacteria that nitrify ammonium to nitrite. *Dendoricella* spp. indet. of the *Halichondria/Dendoricella* cluster host Proteobacteria that might contribute to the ammonification of DOM and *Halichondria* sp. of the same cluster potentially contain ammonia-oxidizing or nitrifying bacteria involved in DNRA and ammonification of DOM. Sponges of the *Lissodendoryx* cluster are LMA sponges that might feed selectively on phytodetritus-derived POC which is subsequently ammonified, but they might also gain metabolic energy from their symbionts. The last investigated LMA sponges belong to the *Tedania* cluster that hosts Bacteroidota which might be able to degrade carbohydrates and contribute to the ammonification of DOM. Additionally, the sponges might contain nitrifying bacteria. In contrast, the *Suberites* cluster sponges are HMA sponges and potentially consume carbohydrates originating from deep-sea coral mucus that are degraded by Chloroflexota. Furthermore, they might ammonificate phytodetritus-based POC. These proposed processes should be confirmed with further experimental studies such as DNA-stable isotope probing (DNA-SIP; e.g. (Campana et al., 2021),)

combined with compound-specific stable isotope analysis (CSIA), and metagenomic data.

CRediT authorship contribution statement

Tanja Stratmann: Writing – original draft, Visualization, Validation, Software, Resources, Project administration, Methodology, Investigation, Funding acquisition, Formal analysis, Data curation, Conceptualization. **Kathrin Busch:** Visualization, Validation, Software, Methodology, Investigation, Formal analysis, Data curation. **Anna de Kluijver:** Writing – review & editing, Methodology. **Michelle Kelly:** Writing – review & editing, Validation, Formal analysis. **Sadie Mills:** Writing – review & editing, Validation, Resources, Data curation. **Sven Rossel:** Writing – review & editing, Validation, Methodology, Investigation. **Peter J. Schupp:** Writing – review & editing, Supervision, Resources, Funding acquisition.

Declaration of competing interests

There are no conflicts of interest declared for this submission.

Data availability

All data presented in this manuscript are available at Pangaea (https://doi.pangaea.de/10.1594/PANGAEA.971483, https://doi.pangaea.de/10.1594/PANGAEA.971489, https://doi.pangaea.de/10.1594/PANGAEA.971487), on GenBank (accession numbers of sponge data are presented in Table S1), and NCBI (accession numbers: PRJNA1102912; http://www.ncbi.nlm.nih.gov/bioproject/1102912). Molecular genetic data are deposited in the barcode of life data system (BOLD) in the project Sponges off New Zealand (SONZ) and processed mass spectrometry data can be found in Supplementary Data S1.

Sample collection was carried out under the "Application for consent to conduct marine scientific research in areas under national jurisdiction of New Zealand (dated June 7, 2016)."

Declaration of competing interest

The authors declare that they have no known competing financial interests or personal relationships that could have appeared to influence the work reported in this paper.

This is publication number 21 of Senckenberg am Meer Proteome Laboratory and number 96 of Senckenberg am Meer Metabarcoding and Molecular Laboratory.

Appendix A. Supplementary data

Supplementary data to this article can be found online at https://doi.org/10.1016/j.dsr.2024.104416.

Data availability

The data have been submitted to public repositories.

References

Altschul, S.F., Madden, T.L., Schäffer, A.A., Zhang, J., Zhang, Z., Miller, W., Lipman, D.J., 1997. Gapped BLAST and PSI-BLAST: a new generation of protein database search programs. Nucleic Acids Res. 25, 3389–3402.

Bart, M.C., de Kluijver, A., Hoetjes, S., Absalah, S., Mueller, B., Kenchington, E., Rapp, H. T., de Goeij, J.M., 2020. Differential processing of dissolved and particulate organic matter by deep-sea sponges and their microbial symbionts. Sci. Rep. 10, 17515. https://doi.org/10.1038/s41598-020-74670-0.

Bayer, K., Jahn, M.T., Slaby, B.M., Moitinho-Silva, L., Hentschel, U., 2018. Marine sponges as Chloroflexi hot spots: genomic insights and high-resolution visualization of an abundant and diverse symbiotic clade. mSystems 3. https://doi.org/10.1128/mSystems.00150-18.

Beaulieu, S.E., 2001. Life on glass houses: sponge stalk communities in the deep sea. Mar Biol 138, 803–817. https://doi.org/10.1007/s002270000500.

Bell, J.J., 2008. The functional roles of marine sponges. Estuar. Coast Shelf Sci. 79, 341–353. https://doi.org/10.1016/j.ecss.2008.05.002.

Bligh, E.L.G., Dyer, W.J.A., 1959. A rapid method of total lipid extraction and Purification. Can. J. Biochem. Physiol. 37, 911–917. https://doi.org/10.1139/o59-099.

Bolyen, E., Rideout, J.R., Dillon, M.R., Bokulich, N.A., Abnet, C.C., Al-Ghalith, G.A., Alexander, H., Alm, E.J., Arumugam, M., Asnicar, F., Bai, Y., Bisanz, J.E., Bittinger, K., Brejnrod, A., Brislawn, C.J., Brown, C.T., Callahan, B.J., Caraballo-Rodríguez, A.M., Chase, J., Cope, E.K., Da Silva, R., Diener, C., Dorrestein, P.C., Douglas, G.M., Durall, D.M., Duvallet, C., Edwardson, C.F., Ernst, M., Estaki, M., Fouquier, J., Gauglitz, J.M., Gibbons, S.M., Gibson, D.L., Gonzalez, A., Gorlick, K., Guo, J., Hillmann, B., Holmes, S., Holste, H., Huttenhower, C., Huttley, G.A., Janssen, S., Jarmusch, A.K., Jiang, L., Kaehler, B.D., Kang, K. Bin, Keefe, C.R., Keim, P., Kelley, S.T., Knights, D., Koester, I., Kosciolek, T., Kreps, J., Langille, M.G. I., Lee, J., Ley, R., Liu, Y.-X., Loftfield, E., Lozupone, C., Maher, M., Marotz, C., Martin, B.D., McDonald, D., McIver, L.J., Melnik, A.V., Metcalf, J.L., Morgan, S.C., Morton, J.T., Naimey, A.T., Navas-Molina, J.A., Nothias, L.F., Orchanian, S.B., Pearson, T., Peoples, S.L., Petras, D., Preuss, M.L., Pruesse, E., Rasmussen, L.B., Rivers, A., Robeson, M.S., Rosenthal, P., Segata, N., Shaffer, M., Shiffer, A., Sinha, R., Song, S.J., Spear, J.R., Swafford, A.D., Thompson, L.R., Torres, P.J., Trinh, P., Tripathi, A., Turnbaugh, P.J., Ul-Hasan, S., van der Hooft, J.J.J., Vargas, F., Vázquez-Baeza, Y., Vogtmann, E., von Hippel, M., Walters, W., Wan, Y., Wang, M., Warren, J., Weber, K.C., Williamson, C.H.D., Willis, A.D., Xu, Z.Z., Zaneveld, J.R., Zhang, Y., Zhu, Q., Knight, R., Caporaso, J.G., 2019. Reproducible, interactive, scalable and extensible microbiome data science using QIIME 2. Nat. Biotechnol. 37, 852–857. https://doi.org/10.1038/s41587-019-0209-9.

Bowerbank, J.S., 1858. On the anatomy and physiology of the spongiadae. Part I. On the Spicula. Philos. Trans. R. Soc. 148 (2), 279–332.

Burgsdorf, I., Sizikov, S., Squatrito, V., Britstein, M., Slaby, B.M., Cerrano, C., Handley, K. M., Steindler, L., 2022. Lineage-specific energy and carbon metabolism of sponge symbionts and contributions to the host carbon pool. ISME J. 16, 1163–1175. https://doi.org/10.1038/s41396-021-01165-9.

Busch, K., Slaby, B.M., Bach, W., Boetius, A., Clefsen, I., Colaço, A., Creemers, M., Cristobo, J., Federwisch, L., Franke, A., Gavriilidou, A., Hethke, A., Kenchington, E., Mienis, F., Mills, S., Riesgo, A., Ríos, P., Roberts, E.M., Sipkema, D., Pita, L., Schupp, P.J., Xavier, J., Rapp, H.T., Hentschel, U., 2022. Biodiversity, environmental drivers, and sustainability of the global deep-sea sponge microbiome. Nat. Commun. 13. https://doi.org/10.1038/s41467-022-32684-4.

Busch, K., Wurz, E., Rapp, H.T., Bayer, K., Franke, A., Hentschel, U., 2020. Chloroflexi dominate the deep-sea Golf Ball sponges Craniella zetlandica and Craniella infrequens throughout different life Stages. Front. Mar. Sci. 7. https://doi.org/10.3389/fmars.2020.00674.

Callahan, B.J., McMurdie, P.J., Rosen, M.J., Han, A.W., Johnson, A.J.A., Holmes, S.P., 2016. DADA2: high-resolution sample inference from Illumina amplicon data. Nat. Methods 13, 581–583. https://doi.org/10.1038/nmeth.3869.

Campana, S., Busch, K., Hentschel, U., Muyzer, G., de Goeij, J.M., 2021. DNA-stable isotope probing (DNA-SIP) identifies marine sponge-associated bacteria actively utilizing dissolved organic matter (DOM). Environ. Microbiol. 23, 4489–4504. https://doi.org/10.1111/1462-2920.15642.

Caporaso, J.G., Lauber, C.L., Walters, W.A., Berg-Lyons, D., Lozupone, C.A., Turnbaugh, P.J., Fierer, N., Knight, R., 2011. Global patterns of 16S rRNA diversity at a depth of millions of sequences per sample. Proc Natl Acad Sci U S A 108, 4516–4522. https://doi.org/10.1073/pnas.1000080107.

Carballeira, N., Thompson, J.E., Ayanoglu, E., Djerassi, C., 1986. Biosynthetic studies of marine lipids. 5. The biosynthesis of long-chain branched fatty acids in marine sponges. J. Org. Chem. 51, 2751–2756. https://doi.org/10.1021/jo00364a024.

Cathalot, C., Van Oevelen, D., Cox, T.J.S., Kutti, T., Lavaleye, M., Duineveld, G.C.A., Meysman, F.J.R., 2015. Cold-water coral reefs and adjacent sponge grounds: hotspots of benthic respiration and organic carbon cycling in the deep sea. Front. Mar. Sci. 2, 1–12. https://doi.org/10.3389/fmars.2015.00037.

Conway, K.W., Barrie, J.V., Austin, W.C., Luternauer, J.L., 1991. Holocene sponge bioherms on the western Canadian continental shelf. Cont Shelf Res 11, 771–790. https://doi.org/10.1016/0278-4343(91)90079-L.

Conway, K.W., Barrie, J.V., Krautter, M., 2005. Geomorphology of unique reefs on the western Canadian shelf: sponge reefs mapped by multibeam bathymetry. Geo Mar. Lett. 25, 205–213. https://doi.org/10.1007/s00367-004-0204-z.

Conway, K.W., Krautter, M., Barrie, J.V., Neuweiler, M., 2001. Hexactinellid sponge reefs on the Canadian continental shelf: a unique "living fossil.". Geosci. Can. 28, 71–78.

de Kluijver, A., 2021. Fatty Acid Analysis Sponges. protocols.Io. https://doi.org/10.17504/protocols.io.bhnpj5dn.

de Kluijver, A., Nierop, K.G.J., Morganti, T.M., Bart, M.C., Slaby, B.M., Hanz, U., de Goeij, J.M., Mienis, F., Middelburg, J.J., 2021. Bacterial precursors and unsaturated long-chain fatty acids are biomarkers of North-Atlantic deep-sea demosponges. PLoS One 16, e0241095. https://doi.org/10.1371/journal.pone.0241095.

Diaz, C.M., Rützler, K., 2001. Sponges: an essential component of Caribbean coral reefs. Bull. Mar. Sci. 69, 535–546.

Dohrmann, M., Janussen, D., Reitner, J., Collins, A.G., Wörheide, G., 2008. Phylogeny and evolution of glass sponges (Porifera, Hexactinellida). Syst. Biol. 57, 388–405. https://doi.org/10.1080/10635150802161088.

Duchassaing de Fonbressin, P., Michelotti, G., 1864. Spongiaires de la mer Caraibe. Natuurkundige verhandelingen van de Hollandsche maatschappij der wetenschappen te Haarlem, 21 (2), 1–124.

Engelberts, J.P., Robbins, S.J., de Goeij, J.M., Aranda, M., Bell, S.C., Webster, N.S., 2020. Characterization of a sponge microbiome using an integrative genome-centric approach. ISME J. 14, 1100–1110. https://doi.org/10.1038/s41396-020-0591-9.

Erwin, P.M., Coma, R., López-Sendino, P., Serrano, E., Ribes, M., 2015. Stable symbionts across the HMA-LMA dichotomy: low seasonal and interannual variation in sponge-associated bacteria from taxonomically diverse hosts. FEMS Microbiol. Ecol. 91. https://doi.org/10.1093/femsec/fiv115.

Faergeman, N.J., Knudsen, J., 1997. Role of long-chain fatty acyl-CoA esters in the regulation of metabolism and in cell signalling. Biochem. J. 323, 1–12.

Feuda, R., Dohrmann, M., Pett, W., Philippe, H., Rota-Stabelli, O., Lartillot, N., Wörheide, G., Pisani, D., 2017. Improved modeling of compositional heterogeneity supports sponges as sister to all other animals. Curr. Biol. 27, 3864–3870. https://doi.org/10.1016/j.cub.2017.11.008.

Fiore, C.L., Baker, D.M., Lesser, M.P., 2013. Nitrogen Biogeochemistry in the Caribbean sponge, Xestospongia muta: a source or Sink of dissolved inorganic nitrogen? PLoS One 8. https://doi.org/10.1371/journal.pone.0072961.

Garson, M.J., Zimmermann, M.P., Battershill, C.N., Holden, J.L., Murphy, P.T., 1994. The distribution of brominated long-chain fatty acids in sponge and symbiont cell types from the tropical marine sponge Amphimedon terpenensis. Lipids 29, 509–516. https://doi.org/10.1007/BF02578249.

Gatti, S., Brey, T., Müller, W.E.G., Heilmayer, O., Holst, G., 2002. Oxygen microoptodes: a new tool for oxygen measurements in aquatic animal ecology. Mar Biol 140, 1075–1085. https://doi.org/10.1007/s00227-002-0786-9.

Georgian, S.E., Anderson, O.F., Rowden, A.A., 2019. Ensemble habitat suitability modeling of vulnerable marine ecosystem indicator taxa to inform deep-sea fisheries management in the South Pacific Ocean. Fish. Res. 211, 256–274. https://doi.org/10.1016/j.fishres.2018.11.020.

Gibb, S., 2015. MALDIquantForeign: Import/Export Routines for MALDIquant. A Package for R.

Gibb, S., Strimmer, K., 2012. Maldiquant: a versatile R package for the analysis of mass spectrometry data. Bioinformatics 28, 2270–2271. https://doi.org/10.1093/bioinformatics/bts447.

Giles, E.C., Kamke, J., Moitinho-Silva, L., Taylor, M.W., Hentschel, U., Ravasi, T., Schmitt, S., 2013. Bacterial community profiles in low microbial abundance sponges. FEMS Microbiol. Ecol. 83, 232–241. https://doi.org/10.1111/j.1574-6941.2012.01467.x.

Glasl, B., Robbins, S., Frade, P.R., Marangon, E., Laffy, P.W., Bourne, D.G., Webster, N.S., 2020. Comparative genome-centric analysis reveals seasonal variation in the function of coral reef microbiomes. ISME J. 14, 1435–1450. https://doi.org/10.1038/s41396-020-0622-6.

Gouy, M., Guindon, S., Gascuel, O., 2010. Sea view version 4: a multiplatform graphical user interface for sequence alignment and phylogenetic tree building. Mol. Biol. Evol. 27, 221–224. https://doi.org/10.1093/molbev/msp259.

Graber, S., Sumida, C., Nunez, E., 1994. Fatty acids and cell signal transduction. J. Lipid Mediat. Cell Signal 9, 91–116.

Hallam, S.J., Mincer, T.J., Schleper, C., Preston, C.M., Roberts, K., Richardson, P.M., DeLong, E.F., 2006. Pathways of carbon assimilation and ammonia oxidation suggested by environmental genomic analyses of marine Crenarchaeota. PLoS Biol. 4, 520–536. https://doi.org/10.1371/journal.pbio.0040095.

Hentschel, U., Fieseler, L., Wehrl, M., Gernert, C., Steinert, M., Hacker, J., Horn, M., 2003. Microbial diversity of marine sponges. In: Marine Molecular Bioteochnology. Springer-Verlag, Berlin, 59–8.

Hentschel, U., Usher, K.M., Taylor, M.W., 2006. Marine sponges as microbial fermenters. FEMS Microbiol. Ecol. 55, 167–177. https://doi.org/10.1111/j.1574-6941.2005.00046.x.

Hoer, D.R., Tommerdahl, J.P., Lindquist, N.L., Martens, C.S., 2018. Dissolved inorganic nitrogen fluxes from common Florida Bay (U.S.A.) sponges. Limnol. Oceanogr. 63, 2563–2578. https://doi.org/10.1002/lno.10960.

Hoffmann, F., Radax, R., Woebken, D., Holtappels, M., Lavik, G., Rapp, H.T., Schläppy, M.L., Schleper, C., Kuypers, M.M.M., 2009. Complex nitrogen cycling in the sponge Geodia barretti. Environ. Microbiol. 11, 2228–2243. https://doi.org/10.1111/j.1462-2920.2009.01944.x.

Jiménez, E., Ribes, M., 2007. Sponges as a source of dissolved inorganic nitrogen: Nitrification mediated by temperate sponges. Limnol. Oceanogr. 52, 948–958. https://doi.org/10.4319/lo.2007.52.3.0948.

Kaneda, T., 1991. Iso-and anteiso-fatty acids in bacteria: Biosynthesis, function, and taxonomic significance. Microbiol. Rev. 55, 288–302.

Keesing, J.K., Strzelecki, J., Fromont, J., Thomson, D., 2013. Sponges as important sources of nitrate on an oligotrophic continental shelf. Limnol. Oceanogr. 58, 1947–1958. https://doi.org/10.4319/lo.2013.58.6.1947.

Keller, C., 1889. Die Spongienfauna des rothen Meeres (I. Hälfte). Zeitschrift für wissenschaftliche Zoologie 48, 311–405.

Kelly, J.R., Scheibling, R.E., 2012. Fatty acids as dietary tracers in benthic food webs. Mar. Ecol. Prog. Ser. 446, 1–22. https://doi.org/10.3354/meps09559.

Kelly, Michelle, Sim-Smith, C., 2023. Kingdom Animalia, phylum Porifera (sponges). In: Kelly, M., Mills, S., Terezow, M., Sim-Smith, C., Nelson, W. (Eds.), The Marine Biota of Aotearoa New Zealand. Updating Our Marine Biodiversity Inventory. NIWA Biodiversity Memoir, pp. 84–109.

Kersken, D., Kocot, K., Janussen, D., Schell, T., Pfenninger, M., Martínez Arbizu, P., 2018. First insights into the phylogeny of deep-sea glass sponges (Hexactinellida) from polymetallic nodule fields in the Clarion-Clipperton Fracture Zone (CCFZ), northeastern Pacific. Hydrobiologia 811, 283–293. https://doi.org/10.1007/s10750-017-3498-3.

Kumala, L., Larsen, M., Glud, R.N., Canfield, D.E., 2021. Spatial and temporal anoxia in single-osculum Halichondria panicea demosponge explants studied with planar optodes. Mar Biol 168. https://doi.org/10.1007/s00227-021-03980-2.

Kutti, T., Bannister, R.J., Fosså, J.H., 2013. Community structure and ecological function of deep-water sponge grounds in the Traenadypet MPA-Northern Norwegian continental shelf. Cont Shelf Res 69, 21–30. https://doi.org/10.1016/j.csr.2013.09.011.

Lamarck, J.-B. de., 1814 [1813]. Sur les polypiers empâtés. Annales du Museum national d'Histoire naturelle 20, 294–312.

Landry, Z., Swa, B.K., Herndl, G.J., Stepanauskas, R., Giovannoni, S.J., 2017. SAR202 genomes from the dark ocean predict pathways for the oxidation of recalcitrant dissolved organic matter. mBio 8. https://doi.org/10.1128/mBio.00413-17.

Lawson, M.P., Bergquist, P.R., Cambie, R.C., 1984. Fatty acid composition and the classification of the Porifera. Biochem Syst Ecol 12, 375–393. https://doi.org/10.1016/0305-1978(84)90070-X.

Legendre, P., Gallagher, E.D., 2001. Ecologically meaningful transformations for ordination of species data. Oecologia 129, 271–280. https://doi.org/10.1007/s004420100716.

Lendenfeld, R. von., 1886 [1885]. A Monograph of the Australian Sponges. Part VI. The Genus *Euspongia*. Proceedings of the Linnean Society of New South Wales 10 (3), 481–553.

Lindsay, D.B., 1975. Fatty acids as energy sources. Proc. Nutr. Soc. 34, 241–248. https://doi.org/10.1079/pns19750045.

Linnaeus, C., 1758. Systema Naturae per regna tria naturae, secundum classes, ordines, genera, species, cum characteribus, differentiis, synonymis, locis. Editio decima, reformata, [10th revised edition], vol. 1. Laurentius Salvius, Holmiae, p. 824.

Litchfield, C., Greenberg, A.J., Noto, G., Morales, R.W., 1976. Unusually high levels of C24−C30 fatty acids in sponges of the class demospongiae. Lipids 11, 567–570. https://doi.org/10.1007/BF02532903.

Lüskow, F., Riisgård, H.U., Solovyeva, V., Brewer, J.R., 2019. Seasonal changes in bacteria and phytoplankton biomass control the condition index of the demosponge Halichondria panicea in temperate Danish waters. Mar. Ecol. Prog. Ser. 608, 119–132. https://doi.org/10.3354/meps12785.

Macdiarmid, A.B., Law, C.S., Pinkerton, M., Zeldis, J., 2013. New Zealand marine ecosystem services. In: Ecosystem Services in New Zealand–Conditions and Trends, pp. 238–253.

Mackenzie, A.K., Pope, P.B., Pedersen, H.L., Gupta, R., Morrison, M., Willats, W.G.T., Eijsink, V.G.H., 2012. Two SusD-like proteins encoded within a polysaccharide utilization locus of an uncultured ruminant bacteroidetes phylotype bind strongly to cellulose. Appl. Environ. Microbiol. 78, 5935–5937. https://doi.org/10.1128/AEM.01164-12.

Maldonado, M., Bayer, K., Lopez-Acosta, M., 2024. Nitrogen and Phosphorus Cycling Through Marine Sponges: Physiology, Cytology, Genomics, and Ecological Implications. In: Saleuddin, S., Leys, S.R., Roer, R., Wilkie, I.C. (Eds.), Frontiers in Invertebrate Physiology: A Collection of Reviews. On-Bilaterian Phyla. Apple Academic Press, pp. 197–288.

Maldonado, M., López-Acosta, M., Busch, K., Slaby, B.M., Bayer, K., Beazley, L., Hentschel, U., Kenchington, E., Rapp, H.T., 2021. A Microbial Nitrogen Engine Modulated by Bacteriosyncytia in Hexactinellid Sponges: Ecological Implications for Deep-Sea Communities. Front. Mar. Sci. 8. https://doi.org/10.3389/fmars.2021.638505.

Meesters, E., Knijn, R., Willemsen, P., Pennartz, R., Roebers, G., van Soest, R.W.M., 1991. Sub-rubble communities of Curaçao and Bonaire coral reefs. Coral Reefs 10, 189–197. https://doi.org/10.1007/BF00336773.

Moitinho-Silva, L., Steinert, G., Nielsen, S., Hardoim, C.C.P., Wu, Y.C., McCormack, G.P., López-Legentil, S., Marchant, R., Webster, N., Thomas, T., Hentschel, U., 2017. Predicting the HMA-LMA status in marine sponges by machine learning. Front. Microbiol. 8. https://doi.org/10.3389/fmicb.2017.00752.

Morganti, T.M., Slaby, B.M., de Kluijver, A., Busch, K., Hentschel, U., Middelburg, J.J., Grotheer, H., Mollenhauer, G., Dannheim, J., Rapp, H.T., Purser, A., Boetius, A., 2022. Giant sponge grounds of Central Arctic seamounts are associated with extinct seep life. Nat. Commun. 13, 638. https://doi.org/10.1038/s41467-022-28129-7.

Mueller, C.E., Larsson, A.I., Veuger, B., Middelburg, J.J., van Oevelen, D., 2014. Opportunistic feeding on various organic food sources by the cold-water coral Lophelia pertusa. Biogeosciences 11, 123–133. https://doi.org/10.5194/bg-11-123-2014.

Müller, W.E.G., Li, Jinhe, Schröder, H.C., Qiao, Li, Wang, Xiaohong, 2007. The unique skeleton of siliceous sponges (Porifera; Hexactinellida and Demospongiae) that evolved first from the Urmetazoa during the Proterozoic: A review. Biogeosciences 4, 219–232. https://doi.org/10.5194/bg-4-219-2007.

Muyzer, G., Waal, De, And, E.C., Uitierlinden, A.G., 1993. Profiling of Complex Microbial Populations by Denaturing Gel Electrophoresis Analysis of Polymerase Chain Reaction-Amplified Genes Coding for 16S rRNA. Appl. Environ. Microbiol.

Nardo, G.D., 1833. Auszug aus einem neuen System der Spongiarien,wonach bereits die Aufstellung in der Universitäts-Sammlung zu Padua gemacht ist. In: Isis, oder EncyclopädischeZeitung Coll, pp. 519–523 (Oken: Jena).

O'Brien, P.A., Tan, S., Frade, P.R., Robbins, S.J., Engelberts, J.P., Bell, S.C., Vanwonterghem, I., Miller, D.J., Webster, N.S., Zhang, G., Bourne, D.G., 2023. Validation of key sponge symbiont pathways using genome-centric metatranscriptomics. Environ. Microbiol. 25, 3207–3224. https://doi.org/10.1111/1462-2920.16509.

Oksanen, J., Blanchet, F.G., Friendly, M., Kindt, R., Legendre, P., McGlinn, D., Minchin, P.R., O'Hara, R.B., Simpson, G.L., Solymos, P., Stevens, H.H., Szoecs, E., Wagner, H., 2017. Vegan: Community Ecology Package.

Olivi, G. (1792). Zoologia Adriatica, ossia catalogo ragionato degli animali del golfo e della lagune di Venezia. Bassano [G. Remondini e fl.]. [ix] + 334 + xxxii pp., 9 pls.

Pachiadaki, M.G., Sintes, E., Bergauer, K., Brown, J.M., Record, N.R., Swan, B.K., Mathyer, M.E., Hallam, S.J., Lopez-Garcia, P., Takaki, Y., Nunoura, T., Woyke, T., Herndl, G.J., Stepanauskas, R., 2017. Major role of nitrite-oxidizing bacteria in dark ocean carbon fixation. Science.

Pallas, P.S., 1766. Elenchus zoophytorum sistens generum adumbrationes generaliores et specierum cognitarum succintas descriptiones, cum selectis auctorum synonymis. [book]. Fransiscum Varrentrapp, Hagae, p. 451.

Poiret, J.-L.M., 1789. Voyage en Barbarie, ou Lettres écrites de l'Ancienne Numidie pendant les Années 1785 et 1786, avec un Essai sur l'Histoire naturelle de ce Pays. Deuxième Partie (Alcyonium & Porifera) 56–63.

Preston, C.M., Wu, K.Y., Molinski, T.F., DeLong, E.F., 1996. A psychrophilic crenarchaeon inhabits a marine sponge: Cenarchaeum symbiosum gen. nov., sp. nov. Proc. Natl. Acad. Sci. USA 93, 6241–6246. https://doi.org/10.1073/pnas.93.13.6241.

Quast, C., Pruesse, E., Yilmaz, P., Gerken, J., Schweer, T., Yarza, P., Peplies, J., Glöckner, F.O., 2013. The SILVA ribosomal RNA gene database project: Improved data processing and web-based tools. Nucleic Acids Res. 41. https://doi.org/10.1093/nar/gks1219.

R-Core Team, 2022. R: A Language and Environment for Statistical Computing.

Reiswig, H.M., Kelly, M., 2018. The marine fauna of New Zealand: Euplectellid glass sponges (Hexactinellida, Lyssacinosida, Euplectellidae). NIWA Biodivers. Mem. 130, 118–123.

Rix, L., de Goeij, J.M., Mueller, C.E., Struck, U., Middelburg, J.J., van Duyl, F.C., Al-Horani, F.A., Wild, C., Naumann, M.S., van Oevelen, D., 2016. Coral mucus fuels the sponge loop in warm- and cold-water coral reef ecosystems. Sci. Rep. 6, 18715. https://doi.org/10.1038/srep18715.

Rossel, S., Peters, J., Charzinski, N., Eichsteller, A., Laakmann, S., Neumann, H., Martínez Arbizu, P., 2024. A universal tool for marine metazoan species identification: towards best practices in proteomic fingerprinting. Sci. Rep. 14, 1280. https://doi.org/10.1038/s41598-024-51235-z.

Ryan, C.G., Clayton, E., Griffin, W.L., Sie, S.H., Cousens, D.R., 1988. SNIP, a statistics-sensitive background treatment for the quantitative analysis of PIXE spectra in geoscience applications. Nucl. Instrum. Methods Phys. Res. B 34, 396–402. https://doi.org/10.1016/0168-583X(88)90063-8.

Sampath, H., Ntambi, J.M., 2004. Polyunsaturated fatty acid regulation of gene expression. Nutr. Rev. 62, 333–339. https://doi.org/10.1301/nr.2004.sept.333-339.

Savitzky, Abraham, Golay, M.J.E., 1964. Smoothing and Differentiation of Data by Simplified Least Squares Procedures. Anal. Chem. 36, 1627–1639. https://doi.org/10.1021/ac60214a047.

Schreiber, A., Wörheide, G., Thiel, V., 2006. The fatty acids of calcareous sponges (Calcarea, Porifera). Chem. Phys. Lipids 143, 29–37. https://doi.org/10.1016/j.chemphyslip.2006.06.001.

Schmidt, O., 1870. Grundzüge einer Spongien-Fauna des atlantischen Gebietes. Wilhelm Engelmann, Leipzig iii-iv, 1-88, pls I-VI.page(s): 14-15.

Simion, P., Philippe, H., Baurain, D., Jager, M., Richter, D.J., Di Franco, A., Roure, B., Satoh, N., Quéinnec, É., Ereskovsky, A., Lapébie, P., Corre, E., Delsuc, F., King, N., Wörheide, G., Manuel, M., 2017. A large and consistent phylogenomic dataset supports sponges as the sister group to all other animals. Curr. Biol. 27, 958–967. https://doi.org/10.1016/j.cub.2017.02.031.

Soetaert, K., Petzoldt, T., Meysman, F.J.R., 2010. marelac: Tools for Aquatic Sciences. R package version 2.1.

Southwell, M.W., 2007. Sponges Impacts on Coral Reef Nitrogen Cycling, Key Largo, Florida (PhD Thesis). University of North Carolina, Chapel Hill.

Southwell, M.W., Weisz, J.B., Martens, C.S., Lindquist, N., 2008. *In situ* fluxes of dissolved inorganic nitrogen from the sponge community on Conch Reef, Key Largo, Florida. Limnol. Oceanogr. 53, 986–996. https://doi.org/10.4319/lo.2008.53.3.0986.

Spalding, M.D., Fox, H.E., Allen, G.R., Davidson, N., Ferdaña, Z.A., Finlayson, M., Halpern, B.S., Jorge, M.A., Lombana, A., Lourie, S.A., Martin, K.D., McManus, E., Molnar, J., Recchia, C.A., Robertson, J., 2007. Marine ecoregions of the world: A bioregionalization of coastal and shelf areas. Bioscience 57, 573–583. https://doi.org/10.1641/B570707.

Spector, A.A., Yorek, M.A., 1985. Membrane lipid composition and cellular function. J. Lipid Res. 26, 1015–1035.

Steinert, G., Busch, K., Bayer, K., Kodami, S., Arbizu, P.M., Kelly, M., Mills, S., Erpenbeck, D., Dohrmann, M., Wörheide, G., Hentschel, U., Schupp, P.J., 2020. Compositional and Quantitative Insights Into Bacterial and Archaeal Communities of South Pacific Deep-Sea Sponges (Demospongiae and Hexactinellida). Front. Microbiol. 11. https://doi.org/10.3389/fmicb.2020.00716.

Stratmann, T., Mevenkamp, L., Sweetman, A.K., Vanreusel, A., van Oevelen, D., 2018. Has Phytodetritus Processing by an Abyssal Soft-Sediment Community Recovered 26 Years after an Experimental Disturbance? Front. Mar. Sci. 5, 59. https://doi.org/10.3389/fmars.2018.00059.

Sun, X., Kop, L.F.M., Lau, M.C.Y., Frank, J., Jayakumar, A., Lücker, S., Ward, B.B., 2019. Uncultured Nitrospina-like species are major nitrite oxidizing bacteria in oxygen minimum zones. ISME J. 13, 2391–2402. https://doi.org/10.1038/s41396-019-0443-7.

Thiel, V., Blumenberg, M., Hefter, J., Pape, T., Pomponi, S., Reed, J., Reitner, J., Wörheide, G., Michaelis, W., 2002. A chemical view of the most ancient metazoa - Biomarker chemotaxonomy of hexactinellid sponges. Naturwissenschaften 89, 60–66. https://doi.org/10.1007/s00114-001-0284-9.

Thurber, A.R., Sweetman, A.K., Narayanaswamy, B.E., Jones, D.O.B., Ingels, J., Hansman, R.L., 2014. Ecosystem function and services provided by the deep sea. Biogeosciences 11, 3941–3963. https://doi.org/10.5194/bg-11-3941-2014.

Topsent, E., 1915. Une *Rossella* des Açores (*Rossella nodastrella* n. sp.). Bulletin de l'Institut océanographique Monaco 303, 1–6.

Vacelet, J., 1975. Étude en microscopie électronique de l'association entre bactéries et Spongiaires du genre Verongia (Dictyoceratida). J. Microsc. Biol. Cell. 23, 271–288.

van Deenen, L.L.M., 1966. Phospholipids and biomembranes. Prog. Chem. Fats Other Lipids 8, 1–127. https://doi.org/10.1016/0079-6832(66)90003-6.

Van Duyl, F.C., Hegeman, J., Hoogstraten, A., Maier, C., 2008. Dissolved carbon fixation by sponge-microbe consortia of deep water coral mounds in the northeastern Atlantic Ocean. Mar. Ecol. Prog. Ser. 358, 137–150. https://doi.org/10.3354/meps07370.

van Duyl, F.C., Lengger, S.K., Schouten, S., Lundälv, T., van Oevelen, D., Müller, C.E., 2020. Dark CO2 fixation into phospholipid-derived fatty acids by the cold-water coral associated sponge Hymedesmia (Stylopus) coriacea (Tisler Reef, NE Skagerrak). Mar. Biol. Res. 16, 1–17. https://doi.org/10.1080/17451000.2019.1704019.

Van Soest, R.W.M., Boury-Esnault, N., Vacelet, J., Dohrmann, M., Erpenbeck, D., De Voogd, N.J., Santodomingo, N., Vanhoorne, B., Kelly, M., Hooper, J.N.A., 2012. Global diversity of sponges (Porifera). PLoS One 7, e35105. https://doi.org/10.1371/journal.pone.0035105.

Webster, N.S., Taylor, M.W., 2012. Marine sponges and their microbial symbionts: Love and other relationships. Environ. Microbiol. 14, 335–346. https://doi.org/10.1111/j.1462-2920.2011.02460.x.

Weiss, R.F., 1970. The solubility of nitrogen, oxygen and argon in water and seawater. Deep-Sea Res. Oceanogr. Abstr. 17, 721–735. https://doi.org/10.1016/0011-7471(70)90037-9.

Zea, S., 1993. Cover of sponges and other sessile organisms in rocky and coral reef habitats of Santa Marta, Colombian Caribbean Sea. Caribb. J. Sci. 29, 75–88.